GIS-Based Modeling of Debris Flows in Banff National Park, Alberta

by

Eric A. R. Saczuk

A Thesis Submitted to the Faculty of
Graduate Studies in Partial Fulfillment of
the Requirements for the Degree of

Master of Arts

Department of Geography
University of Manitoba
Winnipeg, Manitoba

THE UNIVERSITY OF MANITOBA

FACULTY OF GRADUATE STUDIES

*****

COPYRIGHT PERMISSION PAGE

GIS - BASED MODELING OF DEBRIS FLOWS IN BANFF NATIONAL PARK, ALBERTA

BY

ERIC A. SACZUK

A Thesis/Practicum submitted to the Faculty of Graduate Studies of The University of Manitoba in partial fulfillment of the requirements of the degree

of

MASTER OF ARTS

Abstract

Debris flows are rapid movements of water, rock debris and vegetation down confined channels. Based on field examinations of these channels, a review of current literature and eyewitness accounts of the processes, it is evident that debris flows pose a significant risk to roads, structures and the increasing number of visitors entering Banff National Park. In order to help the Park identify potentially hazardous areas, a GIS database of the locations and attributes of these channels has been developed along with a recurrence interval model. Mode 1 of the model assigns hazard ratings to sites, which may become unstable given predetermined short-term atmospheric conditions. Mode 2 calculates the absolute recurrence interval for an event of given magnitude for each site.

Measurements from digitized aerial photographs were evaluated and employed in the recurrence interval model. Photo interpretation skill was important in reducing variance in measurements made. 12 of 22 sites are currently assigned a high hazard rating and a further 8 sites require between 5 and 93 years to reach a high hazard rating. Mean recurrence interval for each site is 64±6 years based on a 20,000m^3 event.

Further research regarding rate of rock erosion and meaningful threshold volumes is required. Spatial distribution of meteorological stations for the Park needs to be improved in order to precisely establish the factors which lead to debris flow failure.

Acknowledgements

The author would first like to thank those who were directly responsible for making this thesis a reality; Dr. James Gardner who through subtle words of encouragement instilled in me a deep respect for mountain environments, Dr. Michael Campbell who more than once lent a seasoned ear and offered invaluable advice, Dr. David Barber who despite a million better things to do, guided me along the way and saw to it that I didn't stray too far, and last but certainly not least, Dr. Jim Teller who helped me smooth out the rough edges of this thesis.

The University of Manitoba through Dr. Gardner provided financial and logistical support. David Gilbride, Darrel Zell, and Charlie Pacas of the Banff National Park Warden Service granted support in the field in the form of invaluable data and for this the author is grateful. Fes deScally deserves a special thank-you for all the sound advice and allowing me to tag along with him in the field. Anna Preis, Rod Lastra, Tobi Gardner and Dave Burwash also deserve a generous thank-you for their assistance in the field.

The Centre for Earth Observation Science (CEOS) supported this research through access to computer facilities and technical support. In particular the author would like to thank David Mosscrop and Ron Hempel for their technical and moral support throughout the project.

Last but not least I would like to express my infinite gratitude to my mom and dad without whom I would not have gotten very far.

Table of Contents

List of Figures

List of Tables

Chapter I Introduction and Previous Research

1.0 Purpose

Mass wasting processes occur frequently in mountain environments. These environments also are sometimes centers of population concentrations. Humans occupy mountainous areas for varied reasons such as lack of other suitable land, to harvest timber, extract minerals, and to seek recreation. Mountain passes also serve as important transportation corridors linking communities. This juxtaposition of mass wasting processes and human presence creates a potential for natural hazards. Snow-avalanches, floods, landslides, debris flows and rockfall activity all represent a hazard to people travelling in or occupying mountain environments.

Of the hazards mentioned above, debris flows are spatially concentrated and may have high temporal frequencies. They may occur near built structures such as roads or buildings, which are often situated on or near debris flow fans.

Debris flows must be understood in terms of location, magnitude, frequency, release factors, materials, mode of transport, and deposition in order to understand and reduce the risk they pose to humans. A method for efficiently acquiring, organizing and applying these data for

the mitigation of risk could result in greater safety for visitors and residents of mountain environments. This thesis addresses this issue.

1.1 Objectives

The three main objectives of this thesis are:

1) To evaluate the feasibility of using digitized aerial photos and global positioning system (GPS) technology to remotely collect data on debris flow-prone channels in Banff National Park;
2) To use the data to develop a recurrence interval model for debris flows in Banff National Park; and
3) To organize the data into a comprehensive geographic information systems (GIS) debris flow database and map for Banff National Park.

1.2 Thesis presentation

The thesis is organized into 4 chapters. A brief explanation of the content of each chapter is given below.

Chapter 1 introduces the general aim of the paper as stated above. Each of the three objectives is outlined and the presentation of the thesis is explained. Debris flows are defined and a thorough explanation of their characteristics is given with reference to previous literature. An examination of current approaches to studying debris flows is also presented and leads to the justification for this research.

Chapter 2 is a detailed description of the methods used to select the study site, and to gather, organize, and analyze the data.

Chapter 3 presents the results with specific reference to each of the three objectives. A discussion of the results and the propagation of errors is included.

Chapter 4 summarizes the methods and results and states the conclusions in the context of the three objectives. Following the conclusions is a section outlining the need for further research.

1.3 Overview of debris flow research

In this chapter debris flow definitions and terminology, site characteristics, triggering mechanisms, propagation theories, deposition characteristics, and mitigation measures are discussed with reference to previous literature. This is followed by a summary of the current state of research regarding debris flow recurrence intervals, application of remotely acquired data for the purpose of debris flow mitigation, and the use of digital databases to identify debris flow prone locations and characteristics. The chapter ends with a justification for this thesis based on a review of the current state of debris flow research.

1.3.1 Definitions and terminology

Debris flows occur in many different parts of the world including the US (Chen, 1987, Wieczorek, 1987, Benda and Cundy, 1990, Neary and Swift, 1987, Coe *et al.*, 1997, Butler, 1996 and many others), Canada (Hungr *et al.*, 1984; 1987, Luckman, 1997, Jackson *et al.*, 1987, Church, 1984, Slaymaker, 1990, Desloges and Gardner, 1984, Cruden, 1985 and others), Europe (Irigaray, *et al.*, 1994, van Steijn, 1995, Rebetez, 1997 and others) and Asia (Hearn and Jones, 1986, Vuichard, 1986 and others). Many different terms and definitions have been applied to debris flows. Brunsden (1979 *in* Innes, 1983) states that the current debris flow terminology and classifications are inadequate. Table 1.0 summarizes the different terms used to describe debris flows and the authors who initiated the term.

Table 1.0. Terms used to describe debris flows.[1]

Summer solifluction	Baird and Lewis (1957)
Debris avalanche	Williams and Guy (1973)
Debris slide	Bogucki (1977); Rapp (1963)
Debris torrent	Swanston and Swanson (1976)
Lahar	Scrivenor (1929); Neall (1976)
Mud avalanche	Conway (1893;1894)
Mudflow	Blackwelder (1928); Owens (1973; 1974)
Mudrock flow	Bailey *et al.* (1 934)
Mudspate	Rickmers (1913)
Mudstream	Bonney (1902); Scrivenor (1929)
Schlammstrom	Penck (1924)
Debris flow	Varnes (1978)

[1]Based partly on Sharpe (1938) and Pierson (1980) *from* Innes (1983).

The terms in the above table describe the various types of erosion processes occurring on hillslopes for different parts of the world. Many have similar characteristics to debris flows and this indicates that there is little consensus on what a debris flow is and how it is defined amongst researchers in this field (Coussot and Meunier, 1995). VanDine (1985) defines a debris torrent as "a mass movement that involves water-charged, predominantly coarse-grained inorganic and organic material flowing rapidly down a steep, confined, preexisting channel." (p. 46). Other authors modify this basic definition with speed thresholds (Curry, 1966 *in* Innes, 1983), slope thresholds (Chandler, 1972 *in* Innes, 1983) scale (volume of debris) (Pierson, 1980, Ownes, 1974, Sulebak, 1969, Innes, 1982, Azimi and Desvareux, 1974, 1983, Macfarlane, 1980 *in* Innes, 1983 and others) and water content (Gol'din and Gyubashevskiy, 1966 and Syanozhetsky *et al.*, 1973 *in* Innes, 1983 and others). A globally applicable debris flow definition cannot be specific in terms of geology, debris volume, triggering mechanism or flow speed. For these reasons the general definition given by VanDine (1985) above is regarded as the best current definition and will be used in the context of this research.

1.3.2 Site characteristics

Debris flows are found mainly in steep 0 or 1st order mountain channels, which exhibit multi-process characteristics (Figure 2.0)

(Jackson *et al.*, 1987 and Desloges and Gardner, 1986). The channels commonly are incised into bedrock above tree line and into unconsolidated deposits at lower elevations. They exhibit some bedrock control above tree line in the form of rock benches and hollows, which may serve as debris reservoirs. The rock benches and hollows are usually composed of more resistant rock than other parts of the channel. Debris flows themselves consist of poorly sorted, matrix-supported deposits (Benda and Cundy, 1990, Major, 1996, Whipple, 1997, Slaymaker, 1990 and others). They are usually identified on the basis of their lobate fan shape with marginal edges of >4° (Jackson *et al.*, 1987), presence of levees along channel banks (VanDine, 1985, Jackson *et al.*, 1987, and others), and evidence of previous activity (Church, 1984, Jackson *et al.*, 1989, van Steijn, 1995 and others). Evidence of previous activity may include scarred tree bark, disturbed or buried vegetation, and the deposits described above. Jackson *et al.* (1987) have also employed Meltons ruggedness number to identify multi-process channels which show debris flow tendencies. This work is based on research originally carried out by Kostaschuk *et al.* (1986) and is described in detail in Chapter 2. Channel dimensions can vary greatly on a local and global scale (Innes, 1983). Debris flow drainage basins are typically small (<10km^2) with relatively steep (>25°) channels and exhibit great local relief (>500m) (Podor, 1992, Desloges, 1982, Jackson *et al.*, 1987). Debris transported within the channel is typically derived from material mass wasted from the head region, the channel bed, and the banks (Figure 1.0) (VanDine, 1985,

Jackson *et al.*, 1987, deScally, 1998, *pers comm.*). Continuous weathering processes such as freeze-thaw activity, exfoliation, and nivation introduce debris into the channel. Rock fragments ranging in size from silt to large boulders, vegetation including trees, water and possibly ice are typical constituents of a debris flow (Figure 1.1) (Major, 1997, Abbot, 1996, *pers comm.*, Shlemon, 1987 and others).

Figure 1.0. Red area indicates release region, yellow, represents the channel and green, the deposition area. (Author).

Figure 1.1. Debris flow channel loaded with rock debris, vegetation and water. (Gardner).

1.3.3 Triggering mechanisms

There are several potential triggers of debris flows, two of which are dominant. The most common trigger mechanism is an abnormally intense rainstorm event (Garland and Olivier, 1993, Church and Desloges, 1984, Shlemon and Wright, 1987, Wieczorek, 1987, Podor, 1992 and many others). Desloges (1982) states that isolated thunderstorms may often stall over a small basin due to topography and lead to extreme precipitation intensities for a short period of time. A prolonged

convective rain event may create favourable antecedent moisture conditions but a high intensity event is usually the trigger factor of debris flows (Janz and Storr, 1977). The second most common triggering mechanism is the rapid melting of snow or ice, typically during spring and early summer (Podor, 1992, Benda and Cundy, 1987, Jackson *et al.*, 1987 and others). Given unusually warm spring conditions, the abundant winter snow cover will rapidly melt and introduce large volumes of runoff into the channels and their tributaries (Innes, 1983 and others). Rarely, snow avalanches may also mobilize a portion of the debris in the channel (deScally, 1997, *pers comm.*). The third mechanism is the bursting of glacially or rock dammed lakes (Jackson, *et al.*, 1989, Rebetez *et al.*, 1997 and others). This is a relatively infrequent phenomenon, however it can lead to large-scale mass wasting events as evidenced by the Cathedral Crags debris flow in 1978 and 1994 (Jackson *et al.*, 1989 and Campbell, 1998, *pers comm.*). Temporary damming of a stream by rockfall or snow avalanche allows a pool of water to form. Pressure builds from the accumulating water which, causes the dam to burst catastrophically and introduces a large volume of water and debris into the channel. The water entrains the *in situ* debris and mass wastes it downslope in the form of a debris flow.

In essence, water is the necessary ingredient, which initiates a debris flow event. More precisely, as water begins to replace the air pockets between adjacent grains, the intergranular pore-pressure rises and shear

strength between grains diminishes (Coussot and Meunier, 1995, Chen, 1987 and Major, 1997 and others). The addition of moisture to grains resting at or near their angle of repose diminishes the cohesive forces between grains and reduces the angle at which the grains can remain stable. Once the friction threshold specified by the shear strength is crossed, the mass begins surging downslope under the force of gravity (VanDine, 1985, Chen, 1987, Takahashi, 1981 and others).

1.3.4 Flow characteristics

A thorough discussion of debris flow movement theories is not within the scope of this thesis and therefore only a general overview of the two dominant theories is given.

Debris flows are generally classified as Newtonian fluids with water and clay content being the main differentiating characteristics of the two movement theories (Coussot and Meunier, 1995 and Innes, 1983).

Takahashi (1978) proposed a model based on Bagnold's (1954) experiments focussing on the interaction of cohesionless particles. In particular, Takahashi (1978) envisioned debris flows as having very little water content and relying primarily on the transfer of energy between solid particles perpendicular to the slope. This allows for the movement of rock fragments *en masse* away from the slope and thus down hill in a turbulent fashion. Flow is sustained through the propagation of energy

between particles. The failure could be initiated by seismic activity, destabilization of the debris by undercutting of the toe or loading of the upper mass of debris by other slope failures. This theory is questioned by Campbell (1990) and Coussot and Piau (1994) on the basis that it has not been backed by field observations and oversimplifies material interactions and outright ignores any presence of water or clay particles.

An alternative theory is the viscoplastic fluid model, which has been confirmed through field experiments by Johnson (1970), Coussot (1992), and Whipple and Dunne (1992). Debris flows in this case contain clay particles and water, which serve to reduce the strength of the mass. The approach here relies on the ability to calculate the yield stress of debris flows in order to predict the conditions that lead to failure and to deposition. Yield stress of the clay particle interaction network, as measured in the field, must be overcome in order to initiate flow (Coussot and Meunier, 1995). The viscoplastic fluid model relies on Bingham's model (1919) in simple cases where shear is occurring parallel to the slope while the Herschel-Bulkley model is used in more complicated scenarios. Both of these models take into consideration the varying solid fractions encountered within a debris flow as well as the presence of water and clay particles as a lubricant. See Coussot and Meunier (1995) for a detailed description of the models.

A debris flow is typically started near the head of the channel where moisture initially begins infiltrating into the debris. Through the processes described in Section 1.3.3, the destabilized mass of debris

begins to exert additional forces on the material downslope and leads to failure of the remaining *in situ* debris. Debris flows exhibit a surging, turbulent motion while flowing downslope (VanDine, 1985, Coussot and Meunier, 1995, Phillips and Davies, 1988 and Abbott, 1997, *pers comm.*). Debris often builds up on rock benches or behind tree dams until sufficient force is generated to overcome these barriers and flow is resumed (Abbot, 1996, *pers comm.*). Experiments and field observations suggest that large boulders (>3m^3) are able to "raft" on top of a dense matrix consisting of fine rock particles and water (Major, 1995, Coussot and Meunier, 1995, Podor, 1992 and others). Motion of debris within the channel is also dictated by complex friction forces working between the grains and the bed and banks of the channel (Benda and Cundy, 1990, Chen, 1987 and Podor, 1992). Debris flows contain 60-90 percent solids by weight according to Johnson (1970) with water accounting for a very small percentage of the total flow (Costa and Jarrett, 1981). Highest velocities have been measured along the center of the channel, near the top of the debris (Shlemon *et al.*, 1987, Major, 1995, Whipple, 1997 and Phillips and Davies, 1988). Debris has been observed to move down the channel in the form of a "plug" with a steep bouldery front that tapers off towards the back of the mass (Abbott, 1996, *pers comm.*, and others). This is often followed by a hypercontentrated slurry of water and fine debris and has been termed "after flow" or "flushing out" by Church and Desloges (1984) and others. The results of this type of motion are the levees, which are composed of coarse material that has been pushed aside

and the larger clasts resting on a matrix of finer grained material after deposition (figure 2.2) (Podor, 1992, Desloges, 1982, deScally, 1998, *pers comm.*, Costa and Jarrett, 1981 and others).

To date no single all-encompassing theory fully describes the truly complex nature of debris flows and all particle interactions occurring therein. According to Coussot and Meunier (1995) more research is required in order to better understand how energy is transferred within granular flows perhaps based on new theories.

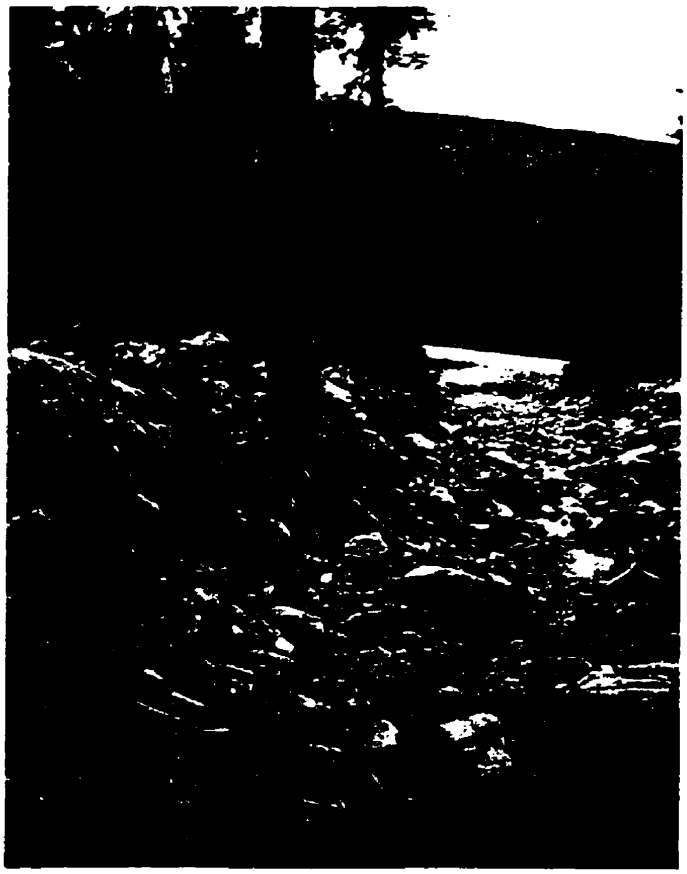

Figure 1.2. Channel with well-developed levees. Notice scaring of tree bark. (Gardner).

1.3.5 Deposition characteristics

As mentioned above, debris flow fan margins tend to be steeper and more convex in plan-view than alluvial fans (Benda and Cundy, 1990 and Jackson, *et al.*, 1987). This is a result of the coarse debris which constitutes a typical debris flow event, the concentration during movement, and the nature of the flow (deScally, 1998, *pers comm.*, Jackson *et al.*, 1987, Teller, 1998, *pers comm.*, and others). Sorting of the debris is often poor and in some cases the deposits are inversely graded (VanDine, 1985 and Major, 1996). This is explained by the matrix-supported nature of debris flows as described above where larger clasts are deposited on a cohesive network of clays, which are able to maintain their strength throughout the flow. Major (1997) carried out several large-scale debris flow flume tests. Based on these tests, Major (1997) concludes that debris tends to accumulate through progressive vertical accretion rather than through *en masse* sedimentation. In the field it is often difficult to distinguish one deposit from another due to the lack of stratigraphy and homogenous nature of the debris (Podor, 1992, Major, 1997 and others).

Deposition can occur on slopes around 10°, but more often on 5° slopes or less and where the channel widens out (VanDine, 1995). Benda and Cundy (1990) found two critical factors, slope less than 3.5° and tributary junction angle greater than 70°, which allowed them to predict the location and runout length of debris flow deposits in the Pacific

Northwest, US. Benda and Cundy (1990) argue that when tributary angles are less than 70°, debris flow deposits tend to enter next-order channels thus increasing the length of their runout.

1.3.6 Mitigative Measures

There are two basic approaches to debris flow hazard mitigation, active and passive. Typically active measures are implemented in areas where debris flows have caused damage and injury or death in the past and where policy and engineering considerations permit construction of mitigative structures. Active measures serve to reduce the volume of potential debris and water and promote deposition in controlled areas. Passive measures are more widely used because they are less expensive to establish and maintain and do not interfere with the natural processes that debris flows represent. They can be considered as warning systems in the form of landuse planning, policy and public education.

Active measures may include the construction of check dams, debris deposition pits, strainers for debris, lining of the channel with concrete, straightening the channel, controlling the source or input of debris, and construction of single-span bridges or fords (VanDine, 1985 and deScally, 1998, *pers comm.*). These structures are constructed based on design-magnitudes, which must be accurately established (Thurber Consultants, Inc., 1985a). Design-magnitudes are based on the maximum volume of debris that a channel is capable of releasing and the potential damage to

structures downslope (Thurber Consultants Inc., 1985a). Japan is very prone to debris flow hazard due to its climate, topography and high population density and also has the most advanced active warning systems in the world (Takahashi, 1981). Europe and Switzerland in particular also have a high spatial density of debris flow channels and many of them are controlled in an active manner (Boll, 1983 *in* VanDine, 1984). In Canada, active measures were not implemented until 1985, when several channels along Highway 99 in British Columbia were modified to reduce the hazard that they posed to several communities near debris flow fans (Thurber Consultants, Inc., 1985b and Church and Desloges, 1984). Passive measures have been implemented in many parts of the world as well. California and Colorado use landuse zoning to prohibit or restrict the erection of structures near known debris flow-prone channels and have set up slope drainage ducts to reduce pore water pressure (Wieczorek, 1987 and Baldwin II *et al.*, 1987).

Very little in the way of active or passive mitigation of debris flow hazard has occurred in other areas of Canada, particularly the eastern Rockies. The National Parks Act specifies minimal human impact on natural processes (Dearden and Rollins, 1993) and therefore active control of debris flows in Banff National Park for example would not generally be possible. However, even passive measures such as warning signs or adequate culverts are non-existent. This is discussed further below.

1.3.7 Recurrence interval methods

The ability to consistently predict when and where debris flows are likely to occur has so far eluded many researchers. In fact several authors have simply concluded that it is not possible to establish when a debris flow will occur at a given site (Church and Desloges, 1984 and Hungr *et al.*, 1984). Despite this, some of the literature attempts to provide a general return period for a specific area or site primarily based on previous debris flow activity. None of these studies have been verified, however, primarily due to the relatively long return periods and complex nature of the process.

Several established methods have been used to try and predict debris flow recurrence intervals. Neary and Swift (1987), Coe *et al.* (1997), Wieczorek (1987), van Steijn (1995), and Garland and Olivier (1993) attempt to establish a return period for their respective debris flow events using a combination of rainfall intensity and antecedent moisture conditions. Most commonly a maximum 24-hr or 3-day rain intensity value is established and used as a threshold beyond which debris flow failure is likely to occur based on previous activity or historical records. Antecedent moisture conditions are taken into account but the effects on debris flow activity are difficult to establish accurately due to variations in soil conditions, which affects rate of infiltration, local drainage patterns, and inaccuracy of meteorological data (Wieczorek, 1987). In

some cases antecedent moisture is simply regarded as present or not present (Neary and Swift, 1987).

Dendrochronology, lichenometry and morphological field investigation of debris flow fan deposits were used to some degree to establish a recurrence interval by Jackson *et al.* (1989), Shlemon *et al.* (1987), Slaymaker (1990), Podor (1992) and Sauchyn (1983). Dendrochronology requires the coring of dead or living trees and an analysis of the growth rings in order to attempt to relatively date the last debris flow event. Lichenometry can also be used to establish the number of years since an event disturbed the fan deposits by measuring lichens growing on rocks and comparing that to established growth rates (Sauchyn, 1983 and Public Works Canada, 1981). A physical analysis of the fan deposits can be used to yield a record of previous activity. However due to the poor stratigraphy of debris flow deposits this is often very difficult and imprecise. This typically involves digging pits in the fan deposits, from which rock fragments are extracted and analyzed based on size, roundness, lithology, and distance from fan edge. This also involves an investigation of the sorting and stratigraphy for evidence of multiple flows (Jackson *et al.*, 1984, Podor, 1992 and others). A temporal series of aerial photos is often used to identify multiple debris flow deposits and arrive at volume estimates (Podor, 1992). Aerial photo and fan deposit methods are hampered by the fact that subsequent debris flows tend to disturb previous inorganic deposits and destroy organic evidence (van

Steijn, 1996 and Major, 1997). These methods are quite field intensive and require time-consuming post-field analysis of the gathered data.

Written records and communication with residents or maintenance crews are sometimes utilized (Podor, 1992 and deScally, 1998, *pers comm.*). However due to the infrequency and incompleteness of many written and verbal records, their usefulness is limited to corroboration of events identified through other methods.

1.3.8 Remotely sensed data in debris flow analysis

Very few current debris flow studies have taken advantage of remotely sensed data to acquire site measurements. Aerial photos are sometimes used to carry out coarse site measurements for the purposes stated above. The resolution of satellite data such as that from Landsat, RadaSat or Spot is often too coarse to carryout measurements of channels but could be used in determining general characteristics such as vegetation, geology and landuse of a basin. Ellen and Mark (1993) utilized a 10m digital elevation model calibrated with historical event data to create a digital map showing hazard in terms of a recurrence interval. They argue that landform is dependent on topography which in turn is a major factor influencing location of debris flow prone areas (Ellen and Mark, 1993). Rowbotham (1995) applied a GIS system to the study of slope instability in Nepal through the use of satellite data. Irigaray *et al.* (1994) also used a GIS with data layers showing tectonic units, lithology,

elevation, slope angle, slope aspect, landforms, rainfall and vegetation to model the occurrence of 4 types of slope movements. Through the use of GIS, Irigaray *et al.* (1994) were able to statistically determine the degree of dependence between the different data layers and type of slope movement.

1.3.9 Debris flow databases

Several authors have attempted to compile a comprehensive database of debris flows for a particular area. Church and Desloges (1984), Thurber Consultants Inc. (1985a and 1985b) and Slaymaker (1990) compiled detailed qualitative and quantitative data on the debris flow channels along Highway 99 in British Columbia. Thurber Consultants Inc. (1985a) carried out an extensive assessment of the debris flow hazard along the Coquihalla Highway (5) in British Columbia. Very detailed data about each channel was gathered and applied to the construction of active mitigation measures at some of the channels (Thurber Consultants Inc., 1985a). Many studies include maps to show the spatial distribution of debris flows but rarely are they accompanied by detailed characteristics of each site. Cruden (1985) states that "No regional program of ... risk mapping has been carried out in the Canadian Cordillera." (p. 536).

1.4 Summary

As the data above suggests, previous attempts at establishing a recurrence interval model have relied heavily on historical data or records of past activity. Some authors have attempted to calibrate their predictive models using a record of previous debris flow activity (Irigaray *et al.*, 1994 and Ellen and Mark, 1993) but in many cases this record is not long enough (<100 years) or not complete enough to be used as an accurate baseline. There is also a discrepancy between which method of determining a recurrence interval works best due mainly to the lack of verified data. Often the data required to build a recurrence model has to be collected in the field, requiring expensive equipment, a source of funding, sufficient manpower, and extensive lab analysis as in the case of dendrochronology and fan deposit analysis. Because of the logistics and time involved with these methods, typically only one or two sites are examined in detail and data for the rest are extrapolated. Detailed rainfall data is a key element in determining the conditions necessary for failure yet many studies rely on coarse 24-hour or 3-day precipitation records. Hourly rainfall data is required in order to accurately establish the precipitation thresholds which lead to debris flow failure (deScally, 1998, *pers comm.*). This leads to a generalization of individual site characteristics and further erodes the accuracy of the recurrence interval model or return period.

This thesis proposes a standard method for collecting pertinent site information using remotely sensed data, organizing these data into a digtial GIS database and map and applying these data to the creation of an accurate recurrence interval model.

Chapter II Methods

2.0 Data collection methods

Four unique sources of data were used for this project; current literature, fieldwork, aerial photo interpretation, and GIS data layers. Aerial photos were evaluated for their usefulness in yielding precise debris flow site measurements because of the potential to acquire most of the variables needed in the recurrence interval model without the need for costly fieldwork. This would allow for a remote analysis of the hazard condition of debris flow channels. Fieldwork was necessary in order to verify aerial photo measurements and to assess the potential for debris flow of each channel. Static or difficult-to-acquire variables were obtained from current literature. Methods used in selecting the study site and collecting and compiling the necessary data are discussed below.

2.0.1 Study area

The study area encompasses all debris flows in Banff National Park, along Highways 1 and 93 (Figure 2.0). Banff Park lies in southwestern Alberta with its western boundary along the eastern border of British Columbia (Figure 2.0). Three major rivers drain the Park; the North Saskatchewan, Mistaya, and Bow (Figure 2.0). These valleys also

coincide with the major thoroughfares in the park and consequently areas of highest debris flow hazard.

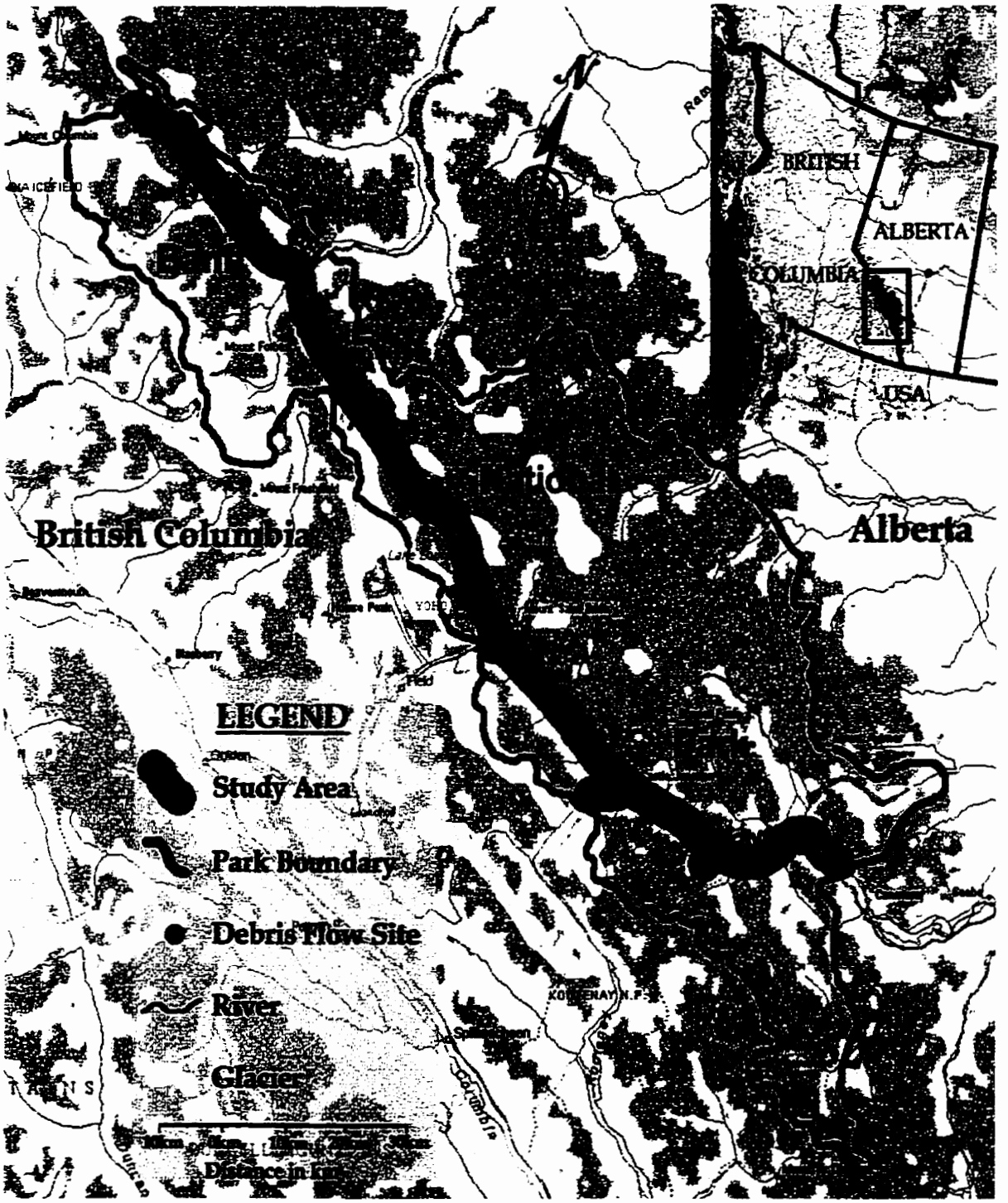

Figure 2.0. Study area showing location of debris flow sites identified during this study.

2.0.2 Geology

Banff Park is divided into two main sub-provinces of the Canadian Rockies, the Front Ranges and Eastern Main Ranges both of which were created during the Columbia orogeny 60 million years ago (Baird, 1974). Geological structure in the front ranges consists mainly of thrust sheets, steeply dipping to the southwest (Halladay and Mathewson, 1971). Stratigraphy of these thrust sheets alternates between erodable Mesozoic siltstone and shale and resistant Late Paleozoic limestone (Figure 2.1) (Price *et al.*, 1971). The resulting landforms are steep northeast facing cliffs where exposure of the strata has led to accelerated erosion of the weak siltstone deposits and gently sloping southwest faces where the slope is almost parallel to the strata. Drainage in the Front Ranges is typically trellis, with short intermittent streams on the northeast slopes and longer perennial channels on the southwest faces (Baird, 1974). The Eastern Main Ranges are eroded into a single, almost flat-lying thrust sheet composed mainly of Precambrian and Early Paleozoic quartzite and limestone (Figure 2.1) (Trenhaile, 1990). The mountains in this sub-province are more massive and of greater relief than those to the east due to the resistant nature of the rock. Drainage here is irregular (Baird, 1974). At least three recent glaciations have eroded and weakened the rock and deposited abundant till along valley floors (Baird, 1974).

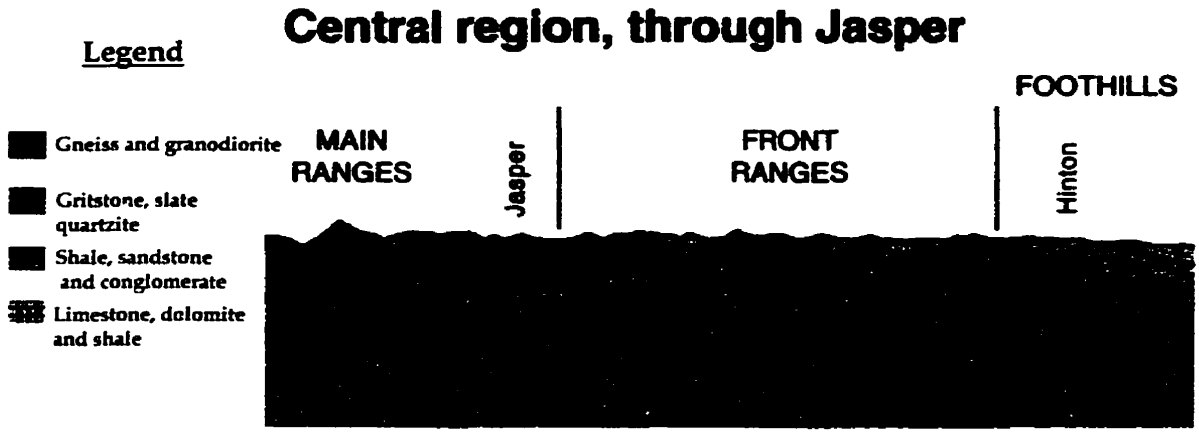

Figure 2.1. Geologic structure and composition of the Front and Eastern Main Ranges of the Canadian Rockies. (Gadd, 1995).

Most of the debris flow hazard sites are located on the southwest-facing slopes of the Eastern Main Ranges (Figure 2.0). This is mainly due to the location of the highway but also because of greater availability of moisture on southwest facing slopes.

2.0.3 Climate and weather

The Rocky Mountains are affected by three dominant air masses; polar continental, polar maritime, and tropical maritime. The climate in the Rockies is described as sub-humid continental or inland (Janz and Storr, 1977). Table 2.0 below provides a summary of the annual temperature and precipitation patterns for the Banff town weather station.

Table 2.0. Average climate data for the Banff town weather station.

AVERAGES	JAN	FEB	MAR	APR	MAY	JUN	JUL	AUG	SEP	OCT	NOV	DEC
Daily High (°C)	-5.3	0.1	3.8	9.0	14.2	18.7	22.1	21.6	16.1	10.1	0.5	-5.3
Daily Low (°C)	-14.9	-11.3	-7.9	-2.8	1.5	5.4	7.4	6.8	2.7	-1.1	-8.2	-13.8
Rainfall (mm)	2.4	1.7	1.6	10.5	42.4	58.4	51.1	51.2	37.7	15.4	6.0	2.8
Snowfall (cm)	38.2	30.0	27.0	26.3	17.1	1.7	0.0	0.0	7.0	18.9	33.6	43.9
Days With Meas. Precip.	12	10	11	11	13	14	13	13	12	9	10	12
Hrs of Sun/Day	8.1	10.0	12.0	14.0	15.5	16.5	16.0	14.5	12.7	10.7	9.0	7.8

(Internet, Parks Canada, 1998).

Winters are generally cool, with abundant snowfall accumulating in October and lasting until June. This pattern is sometimes temporarily modified by chinook winds, which are warm, dry, air masses moving east across the mountains and into the prairies (Brinkmann and Ashwell, 1968 *in* Desloges, 1982). Summers are relatively short with warm temperatures and greatest precipitation in June and July.

Weather patterns in the Canadian Rockies are extremely difficult to generalize. Variability seems to dominate the daily weather. Frost and snow have been detected in all twelve months (Desloges, 1982). Rapid melting of the abundant snow cover may lead to increased runoff rates which may be sufficient to trigger debris flow activity (VanDine, 1985, Jackson *et al.*, 1984, and others). This can occur during late spring or early summer when ice and snow cover is still present in the lower reaches of the basins. Of most importance to this project are the long-duration cyclonic and convective summer storms, which generate locally intense rainstorms of varying duration (Maddox *et al.*, 1977b, and Desloges, 1982). Desloges (1982) found that the frontal overrunning of

warm moist air by cyclogenesis which originated in Montana and moved northward created maximum uplift and thus heaviest rainfalls due to cyclonic activity. Henz (1972) found that an energy surplus created by the heating of south facing slopes lead to the convection of small air masses being pushed upslope by air moving in from the prairies. As the heated air masses continue to rise, they condense into thunderclouds and begin to move eastward according to ambient wind patterns aloft (Orville, 1968). Occasionally topographic barriers will stall a convective system and cause abnormally high precipitation rates in local basins (Desloges, 1982).

2.0.4 Human presence

Natural processes such as debris flows do not constitute a natural hazard without the presence of and potential negative impact on humans and structures. Humans have inhabited this area since the last deglaciation some 8,000 years ago. Currently the Banff Park is under the jurisdiction of Parks Canada, which has a mandate to leave much of the Park in its natural state (Campbell, 1998, *pers comm.*). Despite this, a transportation network consisting of the Trans-Canada Highway, the Canadian Pacific Railway and numerous other paved and gravel roads have been established in the Park. The main reason for this infrastructure was to link British Columbia with the rest of Canada and the mountain passes found in what is now Banff National Park were most

accessible. Two centres, Banff and Lake Louise, with a total population of 8,000 permanent residents, are currently located within the Park boundaries (Pole, 1994). The town of Banff and the hamlet of Lake Louise are not prone to debris flow hazard, however the 5 million annual visitors to the Park (Pacas, 1998, *pers comm.*, and Page *et al.*, 1996), all of whom use the transportation network, are at risk of debris flow activity.

The number of visitors to Banff Park is increasing (Page *et al.*, 1996) and to accommodate the resulting increase in vehicle traffic, the Trans-Canada Highway was twinned in 1997 from Sunshine turnoff to Castle Junction. This exposes more travelers to road-cuts, which are prone to slope-failures. However it also allowed for the expansion of culverts and the erection of single-span bridges at locations where debris flow or fluvial channels come into contact with the highway thus reducing the chance of debris being deposited on the road surface.

A greater debris flow hazard is present along Highway 93 North (Icefields Parkway) due to the higher spatial concentration of active sites. Many tour buses and passenger vehicles use this single-lane road which is the only link between Banff and Jasper Parks through the mountains. Debris flows have blocked traffic and caused property damage to structures near their fans here in the past and the potential to do so in the future remains high mainly due to the inadequate culverts which were designed for water flow and not debris flows.

2.1 Selection of debris flow sites

Twenty-two debris flow-prone channels have been identified for study based on the following criteria:

1) Potential to come into contact with a structure or paved road.
2) Meltons Ruggedness number (r)>0.4 and drainage area between 0.1 and 10km^2.
3) Evidence of previous debris flow activity.

All sites investigated either come into contact with a paved road or show the potential to do so.

Melton's ruggedness number is calculated using the formula

$$r = H_b A_b^{-0.5}$$

where A_b is the basin area and H_b is the basin height. Basin area was measured using aerial photos and basin height was derived from a digital elevation model (DEM) of the Park as described below. Jackson *et al.* (1987) used Melton's ruggedness number to differentiated between sites with multi-process characteristics and those primarily controlled by fluvial activity. For a thorough discussion of Melton's ruggedness number see Kostaschuk *et al.* (1986) and Melton (1965).

A threshold Melton's ruggedness value of r>0.4 was used to distinguish sites dominated by fluvial activity (r<0.4) from multi-process channels that exhibit a tendency to be debris flow controlled (r>0.4) (Jackson, *et al.*, 1987). Drainage basin areas for all sites are between 0.1 and 10km^2. Lack of evidence of previous activity, such as levees, unsorted deposits or tree impact scars, did not disqualify a site if it met the other three criteria. Although debris flow sites were found throughout the park most were concentrated in the northern portion along highway 93 (Figure 2.0). None of the investigated sites have culverts adequate to handle even modest debris flow events. A debris flow event of 500m^3 can completely plug a culvert, which was designed to handle 25-year flood events (Figure 2.2).

Figure 2.2. This 500m^3 debris flow has totally buried a 1.0m culvert, indicated by the arrow. (Gardner).

2.2 Field methods

Field data was gathered during three field seasons; July - September, 1996, July - August, 1997, and June, 1998. Five variables were measured at each of the 22 debris flow channels; width of channel at the highway (W_{Ci}); depth of channel from top of debris (D_{Ei}); diameter of the culvert if present; latitude and longitude, and elevation at the highway. Width of the channel was measured in order to compare it to measurements carried out using aerial photos. This is discussed in detail below. Most of the debris flow channels contained *in situ* deposits and were therefore "loaded" to a certain degree. The depth measurement was taken from the highest point of the debris near the highway to the top of the bank, not including the levee if present (Figure 2.3). This was necessary in order to calculate the current volume of debris. Calculation of the current depth of debris in the channel (D_{Di}) is based on a key assumption about the geometry of 0 or 1st order channels namely, that their cross-sections resemble a right-angle triangle and thus channel depth (D_{Ci}) is one-half the width (W_{Ci}). Therefore;

$$D_{Ci} = 0.5 \times W_{Ci} \text{ and}$$

$$D_{Di} = D_{Ci} - D_{Ei}$$

The right-angle triangle assumption is based on the multi-process origins of these high-order channels which exhibit classic V-shaped cross

sections (Selby, 1982 and Okuda *et al.*, 1980) and was further verified by field observations and previous literature (Figure 2.3) (Johnson, 1970 *in* Podor, 1992).

All measurements were carried out using a standard tape measure. Width and depth values were measured 3 times on three separate occasions and are accurate to ±0.5m and culvert values are ±0.1m. A Magellan Systems Corporation® XL™ global positioning system unit was used to gather latitude, longitude and elevation data. An accurate fix was established by allowing the unit at least 15 minutes to record a position and an elevation reading. It was found that on average, the site position was within 50m of a fix obtained from 1:50,000 topographic maps. This precision was found to be accurate and no further post-mission processing of data was carried out. Elevation data, which were not as important, were found to vary by ±200m due mainly to selective availability and occasional canopy cover, which reduced signal strength.

Several other measurements were taken at selected sites in order to verify assumptions and aerial photo measurements. Channel length (L_{Ci}) was measured using only aerial photos as described below but it was necessary to calibrate these measurements with actual field data. Four sites were chosen and the length of these channels was measured using a Bushnell® Yardage Pro 800™ laser range finder, which has a precision of ±1m. Measurements were taken along straight sections of a channel between two predefined points that were readily identifiable on the aerial photos. Aerial photo values were precise to within ±100m of the

values measured in the field after taking into account slope, which represents 6% of the total average channel length. Another assumption was that the depth of debris, depth of channel and therefore width, remained constant along the length of the channel. The same four sites were used to take W_{Ci} and D_{Ei} measurements at several points along the channels in order to verify this assumption. According to calculations based on research carried out by Thurber Consultants (1985b), the width of the channel at the mouth is within an average of 15% of the width measured at any other point along the channel. This leads to the assumption that the width measured near the highway is representative of the average width of the channel along its entire length within an acceptable standard deviation.

In summary, data gathered during the three field seasons were mainly used for the verification of key assumptions and calibration of remotely gathered data. Only the depth of debris (D_{Di}) variable could not be obtained remotely and had to be measured in the field. Site positions were initially found using a GPS unit but could be obtained by using orthographically corrected and registered aerial photos. Elevation data could be obtained using an existing digital elevation model of the park. A comparison of the elevation values for each site was carried out between the GPS readings, elevations derived from topographic maps, and values obtained from a digital elevation model (DEM) of the Park. It was found that all three data sources were well correlated (Chapter 3).

Figure 2.3. Channel cross-section showing pertinent variables.

2.3 Aerial photo methods

Aerial photos were evaluated for their usefulness in obtaining precise site dimensions based on the experience level of an interpreter. Two experienced interpreters and two inexperienced interpreters each measured the release region areas five times on five randomly selected sites. These data were analyzed using an F-test and a paired T-test to establish whether photo interpretation experience played a role in the precision of site measurements.

Sites were initially located on standard 1:50,000 scale, 1992 monochromatic photos with the help of topographic maps and a GPS unit. Ortho-rectified 1:50,000 digital aerial photos were then used to

carry out channel width (W_{Ci}), length (L_{Ci}) and area of release region (A_{Ri}) measurements.

The digital photos were scanned-in at 600dpi from auto-positives, ortho-rectified, saved in TIF format and copied onto CD-ROM's by the National Air Photo Library in Ottawa. They were then calibrated based on known ground distances and the average pixel resolution was found to be 2.1m, which was sufficient to carry out the necessary measurements.

Sites were located on the digitized aerial photos by referencing the topographic maps and GPS data. Each debris flow site was digitally cropped and saved into a separate file (Figure 2.4 and Appendix 3). In order to carry out the measurements, the cropped photos were first converted to the PSD (PhotoShop™) file format to allow digital layers to be added and the contrast and brightness of each photo was adjusted in order to aid interpretation (Figure 2.4). Adobe® PhotoShop™ allows data to be organized on separate layers, which can then be edited and manipulated individually. Each layer represents one of the three variables being measured (Figure 2.4). Zoom level was adjusted to at least 100% in order to get an accurate measurement. This was due to photo scale and pixel size limits of the software. The pen-tool in Adobe® PhotoShop™ was used to delineate the release area or draw the width and length of the channel on the respective layer. Vector lines were stroked with a raster line a single pixel wide, areas were filled, and a histogram count was selected after all other layers were switched off.

The number of pixels in the histogram was multiplied by the true dimensions of the pixel in order to get a length, width or area measurement. It was apparent that shadows on the photos made measurements difficult to carry out at some sites. In these cases, 1:20,000 color digital photos were used to get more accurate values if a photo of the site was available at the larger scale. The 1:20,000 photos were not used as the primary source of data because they did not cover the study area completely and thus were used mainly as backups for width or length measurements.

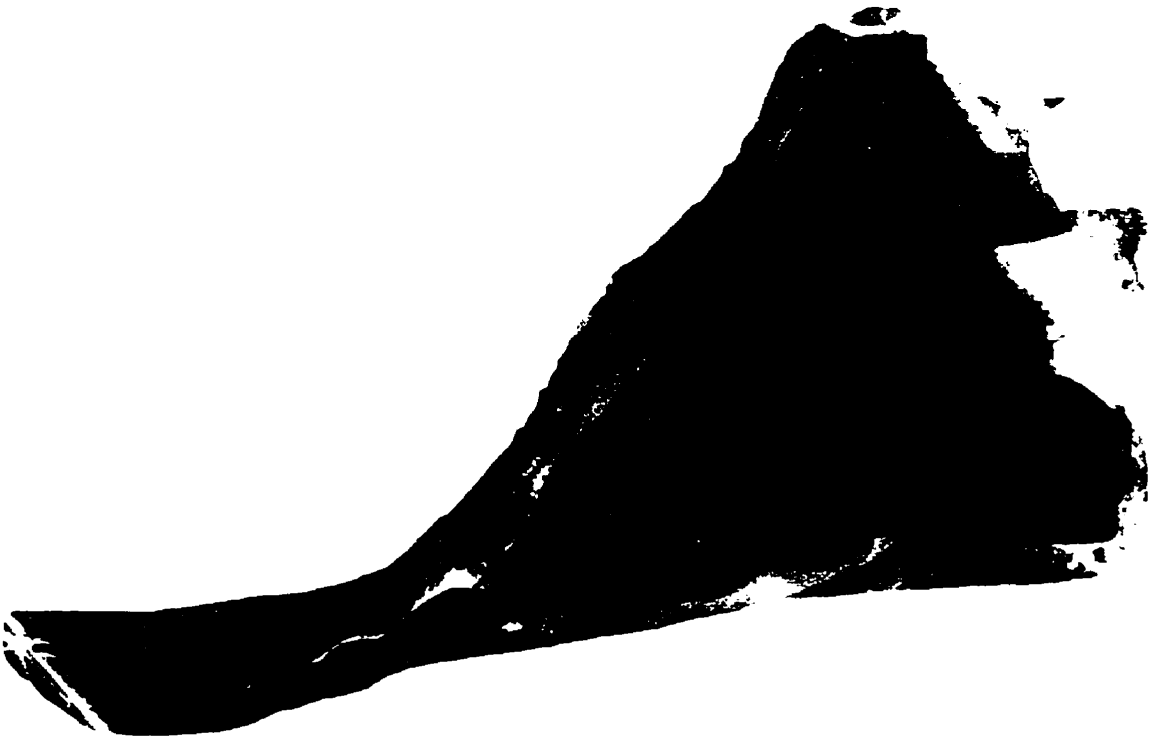

Figure 2.4. Site N93-34 after being cropped, showing release area in purple and channel length in red.

2.3.1 Comparison methods

As mentioned previously it was necessary to assess the agreement between field and photo measurements in order to establish the usefulness of digital photos. Two variables, width (W_{Ci}) and length of the channel (L_{Ci}) were measured in the field as well as on the photos for the purpose of carrying out this agreement assessment. Width of the channel was measured for every site in the field whereas length was measured for only four sites due to logistical limitations. Microsoft® Excel™ v97 was used to carryout a T-test to determine whether the aerial photo measurements were statistically indistinguishable from measurements made in the field.

2.4 Secondary and tertiary data

Several key variables namely T, R_E, and d could not be measured in the field within the time and monetary constraints of this research. A thorough literature review revealed that previous research done on erosion rates (R_E) of certain rock types, threshold volumes (T) and sedimentation rates (d) could be applied to this study area.

Rate of rock erosion (R_E) is a key variable in the recurrence model yet it could not be accurately measured in the field due to the short time-span and limited funding of this research. Therefore results from

previous research carried out in similar geologic and climatic environments were relied upon (Whalley, 1974). Several authors have published figures for erosion rates of rock in the Canadian Rockies (Gadd, 1995, Baird, 1974 and Church, 1984). An average of these (0.0006 ± 0.0001m/year) was used for this research.

Threshold volume of debris was difficult to establish accurately due in part to the lack of volumetric research in this area. A certain volume of debris must accumulate in the channel before a site can be considered a hazard to structures or property downslope as discussed in the previous chapter. Based on a review of typical debris flow deposit volumes, culvert capacities, and previous activity in the Park (Luckman, 1997, Podor, 1992 and Jackson *et al.*, 1989 and 1987), it was determined that a volume of approximately 20,000 ±2,000m^3 of debris in a channel would pose a serious threat to structures downslope. A standard deviation of ±2,000m^3 indicates the relative uncertainty of this variable. Grain size and thus shear strength, slope of the channel, and destabilizing factors are all relatively consistent for all investigated sites and therefore were regarded as a constant.

The variable d represents the percentage of debris that remains in the channel after the annual reworking by fluvial activity. This is an estimate based on the contribution of debris by the debris flow channels to the next order streams such as the Bow River. Previous research indicates that the annual runoff regime does not contribute a significant amount of sediment to next order streams (Selby, 1991 and 1982). Most

of the sediment and debris delivered downslope is a result of episodic events such as debris flows. Table 2.1 shows the variables used in the model, their origins, standard deviation and a short description.

Table 2.1. Variables used in the debris flow recurrence interval model.

Variable	Source	Std. Dev	Description
W_{ch}	Field	0.5m	Width of channel measured in the field
D_{ceh}	Field	0.5m	Depth from top of debris to top of bank
L_{ch}	Photo	100m	Length of channel measured from photos
d	Theoretical	0.1	Percentage of debris left in channel
A_{rd}	Photo	20,000m²	Area of release region for each site
R_E	Theoretical	0.0001m/y	Rate of rock erosion based on previous research
D_{Ch}	$0.5(W_{Ch})$	0.5m	Depth of empty channel
D_{Dh}	$D_{ch} - D_{ceh}$	0.6m	Depth of debris currently in the channel
A_{Ch}	$L_{ch} \times W_{ch}$	1,500m²	Potential area of channel
A_{Dh}	$L_{ch} \times 2(D_{dh})$	1,300m²	Area covered by debris in channel
R_a	$d \times A_r \times R_e$	95m³	Rate of debris accumulation
T	Theoretical	2,000m³	Threshold debris volume
Mode 1	$[T - (D_{dh} \times A_{dh})]/R_a$	12 years	Number of years to reach threshold volume or hazard rating
Mode 2	T/R_a	6 years	Years to threshold for empty channel

2.5 Recurrence interval model

The purpose of obtaining the data described above was to create a comprehensive database, which is described below and to provide values for the formulae in the recurrence interval model. A recurrence interval model is typically used to calculate the period of time between successive events for a given location. In the context of this research, the model was used to establish the hazard rating of each site (Mode 1) and to calculate the number of years between debris flow events of specific magnitude at a given site (Mode 2).

The model developed and used for this research is shown and described in Figure 2.5 below.

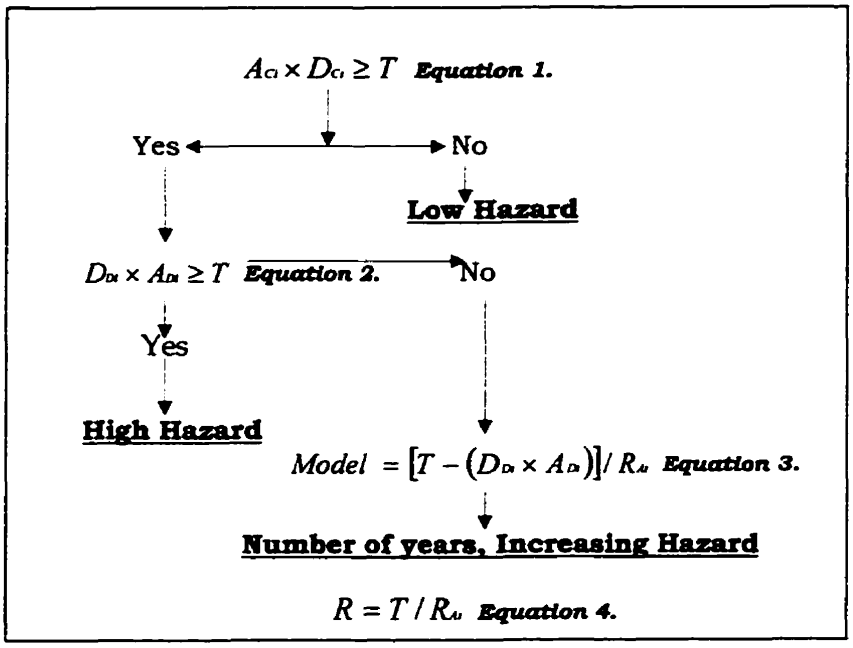

Figure 2.5. Recurrence interval model.

Mode 1 of the model, using **Equations 1, 2, and 3,** assigns a hazard rating to each debris flow site. **Equation 1** assesses whether a channel is able to accommodate the threshold volume (T) based on the area (A_{Ci}) and depth (D_{Ci}) of the channel. If "No" and T cannot be accommodated within the banks of the channel then the site is considered to pose a Low Hazard. If "Yes" then **Equation 2** is used to calculate the current volume of debris using depth of debris (D_{Di}) and area of debris (A_{Di}). If the current volume is equal to or greater than the threshold the site is given a High Hazard rating. If "No", **Equation 3** calculates the number of years it will take to reach the threshold volume by subtracting the current volume

from the threshold and dividing by the annual rate of input of debris from the release area ($d \times A_{Ri} \times R_E$). This is considered a Moderate Hazard site.

In Mode 2, **Equation 4** is used to calculate the number of years required for the channel to reach the threshold volume, assuming an empty channel using threshold (T) divided by annual rate of debris accumulation (R_{Ai}).

All variables are stochastic and, therefore, the output of the model is given as a range of values based on standard deviations of the input data. Microsoft® Excel™ v97 was used to calculate the model outputs as well as the minimum and maximum value for each variable as well as the results. The model framework facilitates easy entry of new or updated variables and automatically recalculates the results based on new data.

2.6 GIS database

The GIS database of all potentially active debris flow sites and their characteristics developed for this area is unique to this type of research. Debris flow inventories have been developed by other authors (van Steijn, 1996, Ellen and Mark, 1993, Church and Desloges, 1984, Irigaray *et al.*, 1994, Thurber Consultants, 1985a and 1985b, and others) however none combine detailed information with the ability to visually locate the site on a digital map. Digital databases are easily updateable and the GIS

environment is well suited to carrying out further analysis and modeling of site variables and characteristics.

2.6.1 GIS hazards map

The debris flow hazards map began as a collection of coordinates for each of the sites identified using the GPS unit. These coordinates were entered into a text file, which was formatted according to a vector data structure for use in Idrisi™ v2.0 software. Each site was represented as a point where the channel comes into contact with a road. However, in order to extract complete site information from other GIS layers, the sites had to be represented as a polygon, which resembled the actual basin dimensions. This was accomplished by creating a mosaic using the aerial photos, which showed the site polygons on a separate layer (Figure 2.6). Once the mosaic was registered to one of the GIS layers, the photo and map layers were turned off leaving only the site polygons. Based on this map, individual layers, one for each polygon, were created in order to extract summary data for each site as described below.

2.6.2 GIS data methods

Seven raster GIS data layers were used to extract site data. Four of these layers were created from a land classification map, which is available from the data manager at the Warden's office in Banff Park.

The remaining three were derived from a digital elevation model of the Park. The layers show ecoregions, landforms, soils, vegetation, aspect, slope and elevation of the Park. The former four are based on an Ecological Land Classification Inventory of the Park carried out during the late 1980's (Natural Resources Canada, 1989). The original paper maps were digitized and linked to a database containing detailed information on the physical attributes of the many ecological units identified during the course of the land classification project (Natural Resources Canada, 1989). The digital maps were subsequently reclassified into the four layers mentioned above in order to facilitate use in this research. A digital elevation model (DEM) created by Banff Park using topographic maps, aerial photos, and differentially corrected GPS data was used to create the aspect and slope maps. All data layers have a pixel resolution of 30m.

The *Overlay* module in Idrisi™ was used to extract data from each of the GIS layers for each of the site polygons. The *Area* module was then used to determine which category was most dominant for each of the seven variables. This information was subsequently entered into the database. These steps were repeated for all sites using all four GIS data layers.

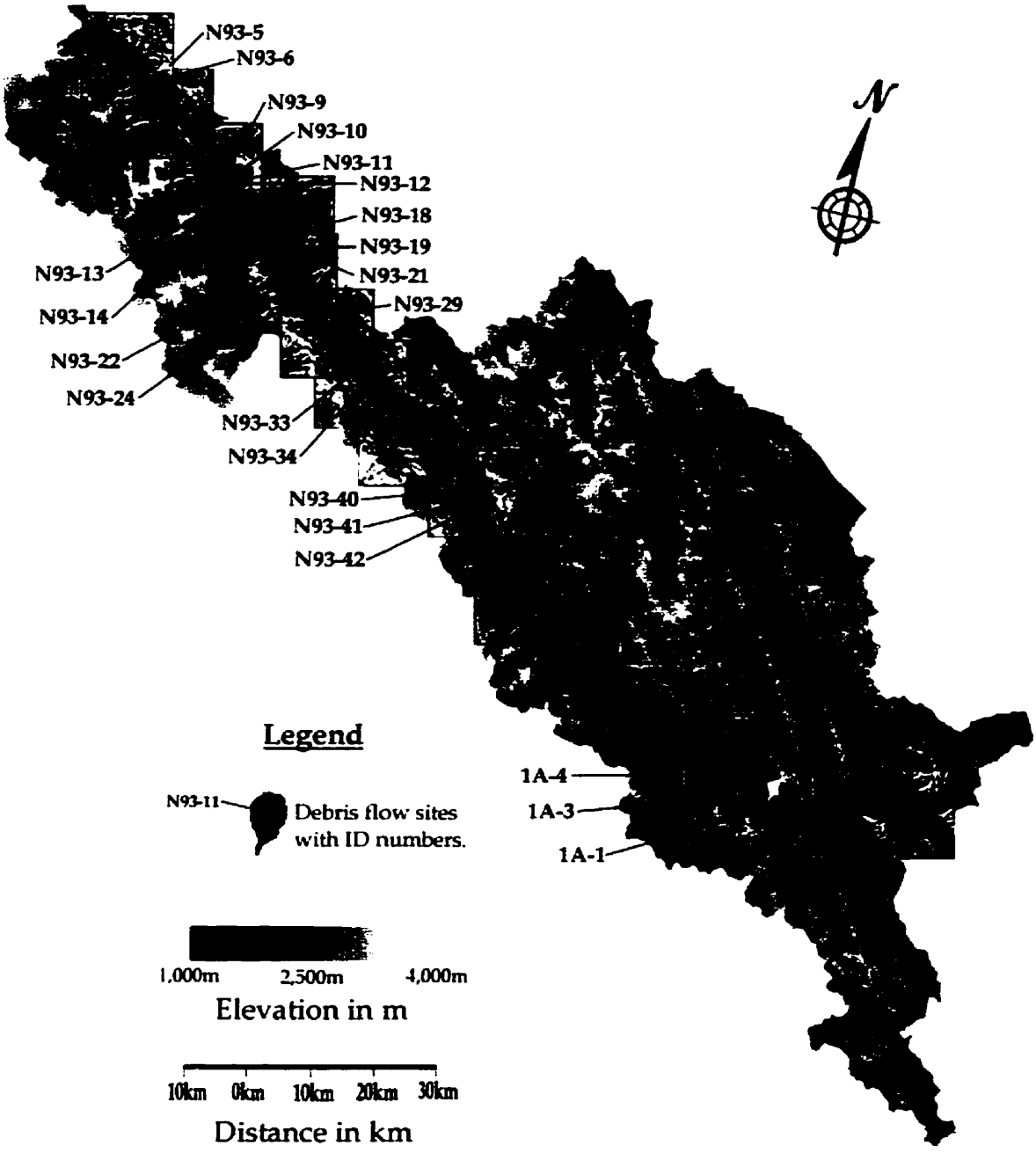

Figure 2.6. Aerial photos registered to a digital elevation model of the Park. Colors are used to indicate the debris flow sites.

2.6.3 Database organization

The database was initially compiled using Microsoft® Excel™ v97 software. All data from the sources described above were organized and entered into the database. The first row and column were used for variable and site identification number, respectively (Appendix 1). Model results are automatically adjusted based on the input variables. The database can easily be translated from Excel™ to Idrisi™ Database Workshop® in order to link it with the hazards map (Appendix 2).

The structure of the database allows it to be easily formatted into many different file formats such as text, space or comma delimited, Microsoft® Access™, dBase® and many others. This is useful if the database is used with other GIS software packages in the future.

2.6.4 Linking hazard map with database

Idrisi™ Database Workshop® allows text files to be imported and converted to the native MS Access™ data format. The only extra step required is to create a column with Idrisi™ identification numbers for each site so that the database entries and the map polygons could be linked using a common identifier. Once a link is established, site characteristics can easily be queried by clicking on their polygon in the map, which then highlights its entry in the database. Variables can easily

be edited and updated in the Workshop® making database maintenance an easy task.

Chapter III Results and Discussion

3.0 Aerial photo results

Digitized aerial photos were registered to topographic maps and evaluated to determine if they could be used to obtain precise channel and basin dimensions. Photo interpretation skill-level was assumed to play a role in the precision of measurements made using these photos.

3.0.1 Photo rectification

The aerial photos were first registered to 1:50,000 topographic maps so that they could be used in Idrisi™ GIS software. The main method of assessing the precision with which the aerial photos were rectified was to check the root mean squared (RMS) value produced by Idrisi™ against the pixel resolution. Typically the RMS value should be lower than the pixel resolution (Lillesand and Kiefer, 1996). However due to the large area, fine resolution of the photos, and precision necessary for measurements, an RMS value of 20m was deemed acceptable. Based on the 17 photos that were rectified, the average RMS was 9.3m. This is well within the accuracy of the GPS unit (±50m) and the pixel resolution of the GIS data layers (30m).

A secondary method of assessing the accuracy with which the aerial photos were registered to topographic maps was to compare the fan locations on the photos to a map of GPS points collected in the field. A vector map of GPS points was overlaid onto the registered photos and a visual inspection confirmed that the point at which the channel comes into contact with the highway coincided on both the photos and vector map for all channels.

3.0.2 Precision of aerial photos

The total variances for both the experienced and inexperienced groups were compared using an F-test. The computed F-statistic of 0.14 is significantly lower than the F-critical value of 4.0 with a corresponding P-value of 0.71. This demonstrates that regardless of the skill level of the interpreter, it is possible to consistently delineate the same area on the photos. Based on this the photos were regarded as being suitable for carrying out precise measurements of release region areas. However it was also found that the total variance of the inexperienced group was higher than the total variance of the experienced group. This indicates that experienced interpreters were able to delineate release areas more precisely and thus may be better suited to making site measurements using aerial photos.

Table 3.0 shows the means of the release areas as measured by the experienced and inexperienced group of interpreters. A T-test revealed

that only the measurements for site N93-29 were statistically indistinguishable between the two groups. The P-values support the T-values and therefore the measurements of the experienced group are statistically different from those of the inexperienced group. Due to the lack of absolute site measurements a statement about measurement accuracy for either group cannot be made.

Table 3.0. Results of a T-test between experienced and inexperienced values[1].

Site No.	Experienced	Inexperienced	T-stat[1]	P-value
1A-1	1,140,979	1,308,020	3.9	0.006
N93-5	600,820	1,060,987	34.5	4.4×10^{-9}
N93-11	792,517	822,953	3.5	0.010
N93-19	1,815,452	1,302,508	-8.6	0.00006
N93-29	534,285	596,509	2.2	0.061

[1]Data in the Experienced and Inexperienced columns show area in m^2 of the release area for each site. [1]T-Crit for two-tailed distribution = 2.4.

Length of channel (L_{Ci}) and width of channel (W_{Ci}) were used to assess the accuracy and precision of measurements made using aerial photos against those made in the field. Table 3.1 below shows the results of a T-test carried out between width measurements made in the field and those made using aerial photos. A T-statistic of -0.14 indicates two data sets are statistically indistinguishable meaning that aerial photo and field measurements are similar. This verifies the usefulness of using aerial photos to carry out channel measurements.

Table 3.1. Average photo and field channel width measurements[1].

Site	Avg. W_{Photo}	Avg. W_{Field}
1A-1	7.0	6.0
N93-5	8.5	7.0
N93-11	13.5	13.5
N93-19	16.0	22.0
N93-29	9.0	8.0
Average	10.8	11.3
T-crit	2.44	
T-stat	-0.14	
P-value	0.88	

[1]Width values are in meters.

3.1 Recurrence model and database results

Results of the recurrence interval model for Mode 1, which assigns a hazard rating to each site, and Mode 2, which establishes the recurrence interval for each site are shown and explained below. This is followed by an explanation of general results gained from the compiled database.

3.1.1 Model mode 1 results

The first operating mode of the model uses a series of simple "if" statement to assign either a high or low hazard rating or the number of years to reach a high hazard rating to each site based primarily on potential channel volume, current debris load and threshold volume. Sites that require a certain number of years to reach the high hazard rating are termed moderate hazard sites in the discussion below. Results for each site are given in Table 3.2 below. The errors of each input

variable were tracked through the model using standard error propagation formulae and displayed as upper and lower risk bounds for each site. The last column in the table below indicates whether the hazard rating of a site changed significantly between the minimum and maximum bounds of the model. For example, if a low hazard rating is assigned to a site under the minimum column but a moderate (number of years) or high hazard rating is shown in the maximum column, then that would constitute a significant change. The reason being is that low hazard sites do not have the potential to accommodate the necessary threshold volume. Moderate hazard sites have the potential to reach the threshold and high hazard sites already contain the minimum volume of debris specified by T.

Table 3.2. Results and the effects of errors on the mode 1 results of the recurrence interval model[1].

Site ID	Mode 1 Results	Mode 1 Min	Mode 1 Max	Change
N93-5	28	58	5	No
N93-6	High Hazard	High Hazard	High Hazard	No
N93-9	Low Hazard	Low Hazard	Low Hazard	No
N93-10	High Hazard	High Hazard	High Hazard	No
N93-11	High Hazard	High Hazard	High Hazard	No
N93-12	High Hazard	High Hazard	High Hazard	No
N93-13	Low Hazard	Low Hazard	Low Hazard	No
N93-14	21	56	High Hazard	Yes
N93-18	High Hazard	High Hazard	High Hazard	No
N93-19	High Hazard	High Hazard	High Hazard	No
N93-21	5	23	High Hazard	Yes
N93-22	High Hazard	High Hazard	High Hazard	No
N93-24	High Hazard	High Hazard	High Hazard	No
N93-29	16	50	High Hazard	Yes
N93-33	High Hazard	High Hazard	High Hazard	No
N93-34	High Hazard	High Hazard	High Hazard	No
N93-40	30	49	16	No
N93-41	93	Low Hazard	50	Yes
N93-42	30	80	High Hazard	Yes
1A-1	26	42	13	No
1A-3	High Hazard	High Hazard	High Hazard	No
1A-4	High Hazard	High Hazard	High Hazard	No

[1]Numerical data is in years.

Based on the above data, 17 of 22 or 77% of the sites remain unchanged regardless of the errors of the input variables. This means that the errors of the input variables do not significantly change the results of the model in the first operating mode.

The data show that of the 22 sites studied there are currently 20 sites that have the potential to fail and 12 sites are currently at or above the threshold level. More importantly only two sites are consistently classified as low hazard within the error bounds of the input variables.

In order to predict when the high hazard sites are most likely to fail, a recurrence interval for a threshold rain event was calculated based on a climatic record for the Park. A recurrence interval of approximately 25 years for a 10mm/hour rain-event indicates that there is a 4% chance that the high hazard sites will fail in any given year. The magnitude of a triggering rain event is dependent on the debris load of the channel. A threshold volume of T = 20,000±2,000m^3 for all channels has been established and based on that, a rain intensity of 10mm/hour for at least 2 hours is required in order to mobilize the debris (deScally, 1998, *pers comm.*, Podor, 1992, Thurber Consultants Inc., 1985a, and Caine, 1980). If the threshold rain event frequency coincides with the time interval required to accumulate the threshold volume, then hazard potential is maximized for that site. However only 3 sites require less than 25 years to accumulate 20,000m^3 of debris, the rest need 30 to 231 years to reach the threshold volume. Thus those sites that have not reached the threshold volume pose a lower, or moderate risk.

3.1.2 Model mode 2 results

The second operating mode is used to calculate the recurrence interval of a particular magnitude event for each site. Again the errors of each input variable were tracked through the equation and the results are accompanied by the minimum and maximum values based on the errors of the input variables (Table 3.3).

From Table 3.3 it is apparent that there is a moderate amount of uncertainty in the recurrence interval for debris flows at each site. The average standard deviation is about 9% of the mean interval, which represents the propagation of error of the input variables. It is interesting to note that the average recurrence interval for all sites is less than 65 years, with one individual interval as low as 18 years. This actually represents a much longer recurrence interval than previously published for this area (Podor, 1992) and is mainly due to a different method of examining each channel and the use of influential variables.

Table 3.3. Mode 2 model results[1].

Site ID	Mode 2	Mode 2 Min	Mode 2 Max	Std. Dev
N93-5	53	47	58	5
N93-6	47	43	52	5
N93-9	60	54	66	6
N93-10	18	16	20	2
N93-11	51	46	56	5
N93-12	73	66	81	7
N93-13	112	100	123	11
N93-14	68	62	75	7
N93-18	23	20	25	2
N93-19	23	21	25	2
N93-21	33	30	37	3
N93-22	231	208	254	23
N93-24	121	109	133	12
N93-29	59	53	65	6
N93-33	68	61	75	7
N93-34	33	30	37	3
N93-40	40	36	44	4
N93-41	117	106	129	12
N93-42	93	84	103	9
1A-1	32	29	35	3
1A-3	25	23	28	3
1A-4	30	27	33	3
Average	64	58	71	6

[1]Data is in years.

3.1.3 Database results

The database compiled during the course of this research is a valuable collection of data on each of the debris flow sites (Appendix 1). It allows for the examination of any relationships that may exist between any two or more variables by simply sorting or plotting the data.

There is an obvious relationship between the variables used to calculate the hazard ratings (D_{Di}, A_{Ci}, A_{Di}, V_{Ci}, and V_{Di}) and the ratings themselves. What's more important however are the thresholds of the variables beyond which a site is considered a high hazard. Table 3.4 below summarizes these threshold values determined from the compiled database.

The mean annual input of debris into each channel was found to be 464 $\pm 95 m^3$ which, in turn, yields an average recurrence interval of 64 years based on an empty channel and a threshold volume of $20{,}000 m^3$.

Table 3.4. Threshold variables used to identify high hazard sites.

Variable	Threshold
Depth of debris (D_{di})	2.5m
Area of channel (A_{ci})	$20{,}000 m^2$
Area of debris (A_{di})	$14{,}000 m^2$
Volume of channel (V_{ci})	$95{,}000 m^3$
Volume of debris (V_{di})[1]	$20{,}000 m^3$

[1]This is the threshold value specified by T.

Sites that are predominantly in the alpine ecoregion have consistently higher ruggedness values ($H_b A_b^{-0.5} = r \geq 0.8$) see Section 2.1. Sites with

$r \leq 0.8$ have a greater percentage of their basin area in the upper subalpine zone. This relationship is based on the fact that the alpine zone tends to have more varied terrain with abundant rock outcrops than lower zones thus making them more rugged.

The dominant soil type found below the treeline at these sites is a mixture of brunisols and regosols. Vegetation along the channel at lower elevations primarily consists of open mixed conifers including pine and buffaloberry as the primary understory which are typically found at disturbed sites. Well-weathered exposed rock faces are the dominant landforms of the sites due to the large release areas, all of which are above tree line. Aspect ranges from 114° to 235° with an average of 185°. This means that most sites are on the southeastern, windward side of the valley, which receives more moisture and more incoming solar radiation than northeast-facing slopes. Slope varies between 24.2° and 41.3° for all the sites and the average of 32° indicates that again a majority of the area of each site is above tree line where slopes are relatively steeper. The average relief of 1270m with a range between 731m and 1638m for all sites is in agreement with previously published data for this region (Desloges, 1982). Drainage area ranges in size from 0.3 to 3.6km^2 and is consistent with basin thresholds published by VanDine (1985)

3.2 Discussion

A discussion of the field methods, aerial photo and database results is presented below.

3.2.1 Discussion of aerial photo results

Registration of the aerial photos to the GIS layers was an important task. It allowed for the remote extraction of site dimensions, from aerial photos, and site characteristics, from GIS maps. These data were used to make general statements about each site as well as the study area as a whole. The precision with which the photos were registered was relatively high and sufficient to carryout the measurements. Fifteen tie-points were used in the registration process which, allowed for a linear or quadratic transformation. The linear transformation yielded an RMS value of 9.3 with three points omitted. The quadratic transformation yielded an RMS of 15 with four points omitted and therefore the linear transformation was applied. The precision of the transformation could have been improved by selecting more points or improving the quality of the existing points. However the RMS value was sufficiently low and no extra steps were taken to improve the precision.

The position where a channel comes into contact with a road on the registered aerial photos was then compared to a vector map of GPS

points collected in the field. The GPS points were found to correspond well with the GIS map positions within several pixels.

Photo interpretation skill level was assessed in order to determine whether it played a significant role in obtaining precise measurements from the photos. This is an important consideration for the acquisition of new data from aerial photos in terms of the skill level requirements of photo interpreters. The photos were found to be useful in carrying out precise measurements of release areas and channel lengths and widths. The total variance for the inexperienced group of interpreters was found to be statistically indistinguishable from the total variance for the experienced group and is a significant finding. It indicates that despite the difference in skill level both groups were able to consistently delineate the release areas precisely. However the inexperienced group had a wider range of variance values (2.3×10^{11}) than did the experienced group (8.3×10^{10}). This seems to indicate that the inexperienced group was less certain of how to identify release areas. For both groups it was found through a debriefing that shadows on the photos, lighting conditions, imprecision in mouse movement and screen resolution all contributed to the uncertainty of the release area boundary. It would be beneficial to obtain aerial photos which, were taken at a time when sun angle was high preferably during the summer months. However due to the long time interval between successive over flights of the same area (average of 8 years) and the limited availability of digitized media it is difficult to obtain such photographs. Errors caused by the imprecision of

the computer mouse and the limitations of the monitor resolution could be minimized by using a more precise input device such as a pen and tablet and a larger (≥21 inch) monitor with finer dot pitch (<0.26).

Four of five basin areas measured by the inexperienced group were found to be statistically different than those measured by the experienced group. However no conclusions can be made about the accuracy with which the basins were measured by either group due to the lack of absolute data with which the measurements made here could be compared.

3.2.2 Discussion of recurrence interval model results

Results for mode 1 of the model show that a 12 of the 22 sites investigated are currently classified as a high hazard. Eight more sites are capable of attaining a high hazard rating but do not currently have the necessary volume of debris and are regarded as a moderate hazard. Only two sites were classified as low hazard.

The 20 sites that are rated as high or moderate hazard have a 4% chance of failing in any given year. This is based on the recurrence interval of a threshold rain event, beyond which failure of the specified volume of debris is likely. The recurrence of this rain event was calculated from an 80-year climate record for the Park (Public Works Canada, 1981). Those sites categorized as low hazard still have the potential to fail, however their inability to accommodate the threshold

volume, T, means that the events will be less significant in terms of damage potential.

As mentioned above the overall recurrence interval for this area is longer than what has previously been published. Podor (1992) stated that the recurrence interval for an event of ~38,000m^3 at West Wilson Creek debris flow (site N93-11) is in the order of 20 years whereas the interval is closer to 50 years for a 20,000m^3 event based on this study. This discrepancy can largely be attributed to differences in establishing the rate of debris accumulation and estimation of previous volume of deposits. Podor (1992) used dendrochronology and fan deposit analysis to establish the recurrence intervals. These methods can be error-prone if not carried out correctly. Conversely this study approaches the problem from a new angle and the methods used here have not been verified in the field. Gardner *in* Desloges (1982) stated that events can be expected to occur every 20 years or so, but did not specify the volume or whether this figure was for one site or all sites in the Eastern Rockies. Based on the results shown above, the average recurrence interval for a 20,000m^3 is in the order of 65 years for any given site and 3 years for all sites combined in any given year. Considering their high spatial concentration this poses a significant risk to structures and people in this region.

3.2.3 Discussion of database and map

The GIS debris flow hazards map layer shows each site as a polygon, which represents its basin area as measured on the aerial photos. This layer can be applied to any of the other 7 GIS data layers in order to create a map showing the sites in the context of the layer data. The main purpose of the map is to visually display the position and configuration of each site relative to other physical features of the Park. It also acts as a query tool allowing for quick extraction of all pertinent site characteristics by clicking on the appropriate site which, then calls up its entry in the database. All GIS layers including the site map have a pixel resolution of 30m which is sufficiently precise to allow undifferentiated GPS points to be plotted for the purpose of further analysis.

The establishment of threshold values beyond which a site is likely to pose a high hazard is important. With the exception of depth of debris (D_{Di}), the other four threshold variables (A_{Ci}, A_{Di}, V_{Ci} and V_{Di}) can be either measured or derived from remotely sensed data (Table 3.4).

Several other relationships help in distinguishing debris flow prone sites from other mountain channels. Buffaloberry typically occupies areas that undergo periodic disturbances and its presence at five of the 12 high hazard sites reinforces that relationship and adds credibility to the GIS vegetation layer (Lastra, 1997, *pers comm.*). Most of the sites are southwest facing, on the eastern slopes of the main valleys, which extend northwest to southeast through Banff Park. This is verified by the

average aspect value of 185°. Site relief is a difficult variable to measure precisely on topographic maps using standard cartographic methods. By overlaying the site map onto a digital elevation model of the Park and running a minimum and maximum filter the relief for each site can be computed precisely. Figure 3.0 below shows a comparison of site elevations measured at the fan of the channel using three different data sources.

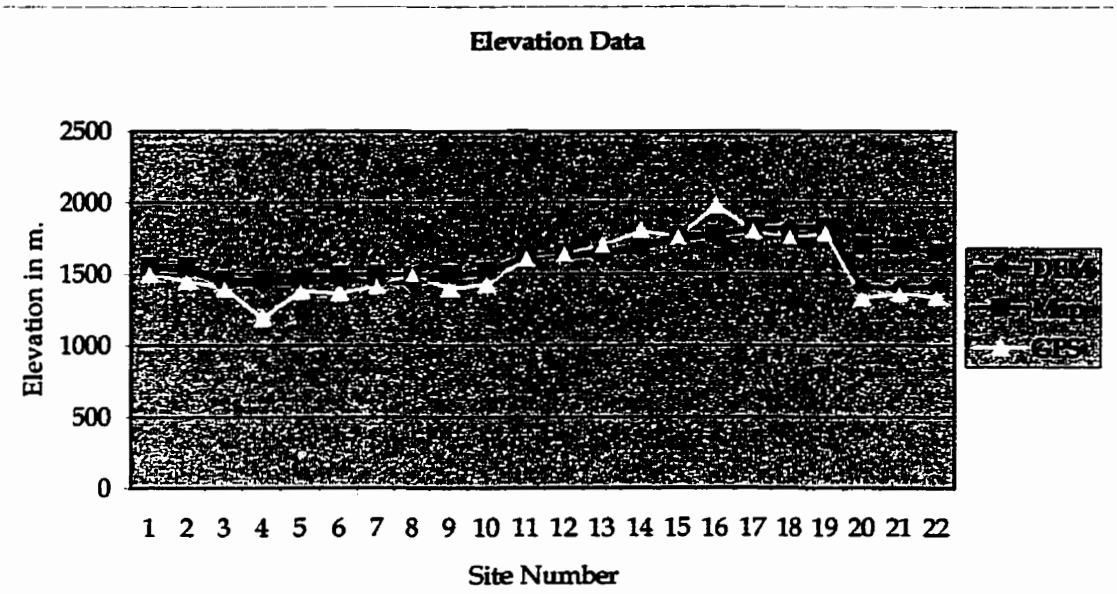

Figure 3.0. Comparison of elevation data from three different sources for each debris flow site.

3.2.4 Discussion of error propagation

The propagation of errors through the model was carefully tracked using standard error propagation formulae in order to ensure that the

errors remained within acceptable limits. The error propagation equations were input into MS™ Excel® v97 and used to compute the errors for each variable. The results of this tracking are represented by the upper and lower limits of the model results. By examining these limits it can be determined which sites pose a consistent hazard and which sites do not. Table 3.2 shows that 17 of the 22 sites remained in the same category regardless of the errors involved.

Excel™ was used to test the effect of each variable and combination of variables on the model results. Variables T, d, and R_E were identified as the biggest contributors of error. This is directly linked to the fact that these three variables are based on previously published data and do not represent primary data. The threshold variable, T, is based primarily on previous debris flow research and thus its standard deviation is difficult to constrain. The d variable is derived from secondary sources and is not specific to the flow regime in the Rockies. R_E is an average value based on local and regional erosion rate research. It represents values obtained through various methods which, have been expressed in depth of material per interval of time.

Despite the errors involved, the results are consistent and precise, although the need for primary data has been acknowledged and is discussed further in the following chapter.

Chapter IV Conclusions

4.0 General goal and objectives of research

The general goal of this research was to develop a method to passively mitigate the hazard that debris flows pose to structures and humans in Banff National Park. The methods developed for this research were also to be applicable to other areas of the world where debris flows represent a hazard.

The three specific objectives of this research were:

1) To evaluate the feasibility of using digitized aerial photos and global positioning system (GPS) technology to remotely collect data on debris flow-prone channels in Banff National Park;
2) To use the data to develop a recurrence interval model for debris flow sites in Banff National Park; and
3) To organize the data into a comprehensive GIS debris flow database and map for Banff National Park.

4.0.1 Objective 1 results and conclusions

The average pixel resolution of the 1:50,000 scale digitized monochrome aerial photos was found to be 2.1m based on verification

data gathered in the field. Fifteen tie-points were used to register each of the 17 photos to a GIS map of the Park. The linear resampling technique yielded an average root mean squared value of 9.3m which is well within the 30m pixel resolution of the GIS layers and ±50m error of the undifferentiated GPS data. A hand-held GPS unit was used to gather accurate site locations and elevations.

The photos were useful in carrying out precise release area and channel length measurements, based on the total intra-interpreter variance, which was assessed using an F-test and P-value. The fact that the total variance was similar for both groups is significant, however variance range was greater for the inexperienced group. This result indicates that aerial photos can be effective for making site measurements but skill level is an important factor to consider. A T-test and the corresponding P-value showed that the release area measurements for the experienced group differed significantly from measurements collected by the inexperienced group for all but one of the 5 randomly chosen test-sites. Table 3.0 summarizes these results.

After the interpreters were debriefed it was found that sun angle and thus shadows on the photos, imprecision of the computer mouse, and monitor resolution all played a role in the accuracy of the measurements. Based on the above results it can be concluded that skilled photo interpreters, working with digitized aerial photos, are able to carryout precise site measurements.

4.0.2 Objective 2 results and conclusions

Results from the first operating mode of the recurrence interval model show that out of the 22 sites examined, 12 are currently considered to be a high hazard, 6 require 5 to 90 years to become a high hazard and 2 are considered a low hazard. The variability of the results was also gauged based on the propagation of the input variable errors. Table 3.1 shows which sites' hazard rating changed from a low hazard to a moderate or high hazard according to the propagation of errors through the model. The results indicate that 77% of the 22 sites studied pose a potential hazard to structures and people downslope with 55% posing a high hazard.

The second mode of the model uses a single equation to calculate the number of years between successive debris flow events of a given magnitude for each site. This recurrence interval is calculated based on a minimum threshold volume and the annual rate at which debris accumulates in each channel. The average interval for all sites is 64 ± 6 years with a range between 18 and 231 years. Based on a rain intensity of 10mm/hr for at least 2 hours failure of the *in situ* debris becomes likely. The recurrence for this rain event is 25years based on an 80-year climate record for the Park. Therefore all sites that are currently at or near the threshold volume of debris have a 4% chance of failure in any given year.

Three variables were based on data from previous literature, T, d, and R_E and thus had correspondingly larger standard deviations than the

primary data collected. As a result, most of the error associated with mode 1 and mode 2 results was attributed to the above three variables, particularly T and R_E.

A recurrence interval model was developed and employed by Banff National Park. The model may be used to monitor and passively mitigate the hazards that debris flows pose to the vehicle traffic on and structures near paved roads in the Park. Model results were derived from data gathered in the field, GIS layers, and current literature and are applied to the identification of potentially hazardous sites. These sites are to be monitored closely by Park personnel when rain intensity, the main triggering factor of debris flows, approaches a predetermined threshold value. Mitigative measures including blocking or rerouting of traffic and clean up procedures can be initiated quicker thus reducing chance of property damage and/or injury.

4.0.3 Objective 3 results and conclusions

The database was useful for extracting general summary information about each individual site and the study area as a whole. Table 4.0 shows the mean and dominant physical characteristics for all sites in the study area.

All data about each site was organized into a digital database as shown in Appendix 1. This database is the most comprehensive collection of information about debris flow sites in Banff National Park.

Its digital nature allows for quick recalculations and entry of new data and it can be linked to a GIS map showing the spatial location of the sites (Appendix 2). Each site on the map is shown as a polygon, which represents the sites' drainage basin. Queries between the map and other GIS layers or between the variables of the database can be carried out easily using Idrisi® GIS or other GIS or database software.

Table 4.0. General debris flow site characteristics.

Variable	Mean/Dominant type	Std. Dev.
D_{cel}	2.1m	0.5m
$W_{cl\ Field}$	11.3m	0.5m
L_{cl}	1,767m	100m
D_{cl}	5.7m	0.5m
D_{dl}	3.5m	0.6m
A_{cl}	20,474m^2	1,468m^2
A_{dl}	13,270m^2	1,316m^2
V_{cl}	158,227m^3	14,118^3
V_{dl}	70,601m^3	9,980m^3
A_{rl}	910,016m^2	20,000m^2
Mode 2	128years	16years
Mode 1	High Hazard	n/a
Ecoregion	Alpine	n/a
Soils	Bruniso, Regosol	n/a
Vegetation	Open Mixed Coniferous	n/a
Landform	Rock	n/a
Aspect	185.7°	5.0°
Slope	32.4°	3.0°
Relief	1270m	100m
Basin Area	1,232,836m^2	20,000m^2
Ruggedness	1.37	0.5

Variables that were dependent on each other were compared in order to yield several key threshold values. Table 3.2 summarizes these values

which, can be used to better understand the conditions necessary for, and physical characteristics of, high hazard debris flows.

4.1 Summary of conclusions

Digitized aerial photos were evaluated and used to measure channel lengths and release areas. Photo interpretation skill was found to be an important factor in obtaining accurate measurements. A Global Positioning System (GPS) unit was useful for collecting accurate site positions and plotting them on digital maps.

A recurrence interval model was developed and used to assess the risk posed by each debris flow site. Twelve of the 22 sites are considered to pose a high level of risk, while a further 8 are considered as potential hazards in the future. Model results are used to identify hazardous sites for the purpose of mitigating the risk that they pose to humans and structures that are in proximity to paved roads in Banff National Park. Average recurrence interval of a 20,000m^3 event for any site is 64±6 years.

Data from literature, fieldwork and GIS analysis was synthesized into a comprehensive debris flow database. Idrisi® software is used to link the database to a GIS map showing site locations.

4.2 Future work

This section addresses shortfalls and new questions encountered during this research. More accurate data on availability and volume of debris, rate of mass wasting of contributing rock slopes, rainfall intensity threshold and interval, and site dimensions would improve the model results and lead to a better mitigative tool for debris flows. These are discussed in detail below.

4.2.1 Debris transport and accumulation

One of the critical factors in the ability to determine how often a site is likely to fail, is the rate of debris accumulation in the channel. As discussed previously, there are several sources of debris, namely the release area above tree line, the channel bed, and the adjacent banks. Out of these three, the release area is the largest and thus accounts for a majority of the debris introduced into the channel. However it is difficult to accurately establish what percentage of this mass wasted debris is stored in temporary depositional areas such as on rock benches and in hollows. Furthermore it is also difficult to quantify the contribution of debris made by the channel bed and banks due to a lack of a suitable measurement method. This leads to the generalization that most of the debris originates from the release area and material derived from the bed and banks of the channel is ignored.

Studies spanning several decades would be required in order to get a good understanding of the characteristics of material mass-wasted from the release area. Gardner (1981a, 1982 and 1986) has concluded that rockfalls are relatively frequent in the Canadian Cordillera. DeScally (1998, *pers comm.*) used painted rocks to quantify movements of debris from the source area into a channel.

The volume of debris contributed by the channel bed and banks could be estimated based on detailed channel measurements before and after a failure. If the potential channel volume increased significantly after an event, this would indicate that bed and bank material was eroded and entrained. The actual volume of debris could be quantified if accurate before-failure measurements were available.

There is no single method available for quantifying the volume of debris that enters a debris flow channel annually. However, through long-term, detailed site observations and measurements a better understanding of the total annual input of debris can be attained.

4.2.2 Rate of rock erosion

Rate of rock erosion was derived from previous literature and thus represents a secondary data source. This variable was found to introduce a significant amount of error into the model results based on its large standard deviation of 17% of the mean. By carrying out primary data collection on the rate of rock erosion for each individual site, this source

of error could be significantly reduced. However this type of research is typically very time intensive, costly and often produces biased results.

Previous erosion rate studies have involved methods which directly measure erosion rate by attaching instruments to rock faces. These studies require years of observations and often the instruments introduce a bias into the results by directly contacting the slope that they are measuring (Lee *et al.*, 1994). A method of remotely measuring the rate of rock erosion through the use of high precision lasers would be feasible given sufficient time and funding. Reducing the errors introduced by using secondary data for erosion rates might improve the validity of these results.

4.2.3 Detailed weather data

Banff National Park operates three weather stations at Banff, Lake Louise and Saskatchewan Crossing. Precipitation data at these three locations is collected on an hourly basis thus yielding a high temporal resolution. The spatial distribution is satisfactory, however all stations are located near valley floors. This leads to a bias in terms of altitudinal precipitation variation. Precipitation generally increases with increasing elevation, but some studies have suggested that the reverse may occur in isolated areas of the Rockies (Janz and Storr, 1977). Furthermore detailed precipitation data for areas above treeline is non-existent and is

necessary in order to accurately estimate the rainfall intensities required to initiate debris flows.

Temporary portable weather stations should be installed and setup to remotely send detailed weather information to a computer. This could be directly linked to the debris flow database in order to provide real-time warning of conditions which may lead to debris flow failure.

4.2.4 Detailed site investigation

A thorough examination of each channel, along its entire length, was not possible under the logistical constraints of this project. A detailed investigation of channel width and depth at several points along each channel would lead to a better estimate of potential and current volume of debris. This in turn could be used to assess more accurately the potential for failure of any site by identifying temporary debris storage areas and areas where erosion is accelerated. The ability to quickly estimate the volume of debris in the channel is important. A portable triangular tool could be developed and used to estimate the "loading" of the channel at several points along its length.

4.2.5 Debris flow recurrence and climate change

Recent evidence suggests that global temperatures are rising and that the magnitude of this increase is greater at the poles and in arctic

environments (Barber, 1998, *pers comm.*). Luckman (1997) states that glaciers in the Rockies have receded the most over the last 100 years based on a 300 year record. Abundant unstable till deposits are left at high elevations as a result of this rapid melting of glacial ice and can be easily entrained by melt water or precipitation events.

In conjunction with this is an apparent increase in the cyclonic activity, which leads to more instances of up-slope weather (Gardner, 1998, *pers comm.*). As a result the frequency of short-term high-intensity rainstorm events has increased over the last several decades (Gardner, 1998, *pers comm.*). This combination of events may lead to a potential increase in the availability of debris as well as an increase in the frequency of triggering rain events. The net result would be an increase in the hazard potential posed by the debris flow sites in Banff National Park. This trend is noticeable in other parts of the world as well. Rebetez (1997) states that "...the number of extreme rainfall events capable of triggering debris flows in August and September has increased (for the Swiss Alps)" (p.36).

It is evident that climate change can directly influence erosion processes and based on current literature the risk posed by mass wasting phenomena such as debris flows may increase in the near future. A concentrated effort to minimize this risk will be an important priority for those engaged in mitigation of hazards in mountainous areas.

References

Bagnold, R. A., 1954, Experiments on gravity-free dispersion of large solid spheres in a Newtonian fluid under shear, *in* Proc., Royal Soc. of London, Ser. A, p. 49-63.

Baird, David, M., 1974, A guide to geology for visitors to Canada's National Parks, Macmillan Company of Canada, Ltd., Toronto, 160p.

Baldwin, Joel E., Donley, Howard F., and Howard, Terry R., 1987, On debris flow/avalanche mitigation and control, San Francisco Bay area, California, *in* Reviews in Engineering Geology Vol. VII, p. 223-236.

Benda, Lee, E., and Cundy, Terrance, W., 1990, Predicting deposition of debris flows in mountain channles, *in* Can. Geotech. J., Vol 27, 1990, p.409-417.

Bingham, E. C., and Green, H., 1919, Paint, a plastic material and not a viscous liquid; the measurement of its mobility and yield value, *in* Proc. Am. Soc. Test. Mater., Vol. 19, p. 640-664.

Bloom, Arthur, L., 1990, Geomorphology: A systematic analysis of Late Cenozoic landforms 2ND ed., Prentice Hall, New Jersey, p.175-195.

Butler, David, R., and Malanson, George, P., 1996, A major sediment pulse in a subalpine river caused by debris flows in Montana, USA, *in*, Z. Geomporh. N. F., Vol.40 No.4, p.525-535.

Campbell, C. S., 1990, Rapid granular flows, *in* Annu. Rev. Fluid Mech., Vol. 22, p.57-92.

Caine, Nel, 1980, The rainfall intensity - duration control of shallow landslides and debris flows, *in* Geografiska Annaler, Vol. 62A, p. 23-27.

Chen, Cheng-lung, 1987, Comprehensive review of debris flow modeling concepts in Japan, *in* Geolgoical Soc. of Am. Rev. in Eng. Geology, Vol. VII, p. 13-29.

Church, M., and Desloges, J. R., 1984, Debris torrents and natural hazards of steep mountain channels: east shore of Howe Sound: Dept. of Geography, Vancouver, British Columbia, 83p.

Coe, Jeffrey, A., Glancy, Patrick, A., and Whitney, John, W., 1997, Volumetric analysis and hydrologic characterization of a modern debris flow near Yucca Mountain, Nevada, *in* Geomorphology Vol. 20, p. 11-28.

Costa, John, E., and Jarrett, Robert, D., 1981, Debris flows in small mountain stream channels of Colorado and their hydrologic implications, *in* Bul. Of the Assoc. of Eng. Geologists, Vol. XVIII, No. 3, p. 309-322.

Coussot, P., and Meunier, M., 1995, Recognition, classification and mechanical description of debris flows, *in* Earth Science Reviews 40 (1996): St-Martin-d'Heres, France, p. 209-227.

Coussot, P., and Piau, J. M., 1994, On the behaviour of fine mud suspensions, *in* Rheol. Acta., Vol. 33, p. 175-184.

Coussot, P., 1992, Rheology of debris flows - Study of contentrated dispersions and suspensions, *unpublished Ph.D. thesis,* INPG, Grenoble, France.

Cruden, D. M., 1985, Rock slope movements in the Canadian Cordillera, *in* Can. Geotech. J., Vol. 22, p. 528-540.

Dearden, Philip, and Rollins Rick, 1993, Parks and protected areas in Canada: Planning and management, Oxford University press, Toronto, 336p.

Desloges, Joseph, R., 1982, Sedimentology and paleohohydrology of alpine multiple-process channels in southwestern Alberta, *unpublished Masters thesis,* University of Wisconsin, Madison, 216 p.

Desloges, Jospeh, R., and Gardner, J., 1984, Process and discharge estimation in ephemeral channels, Canadian Rocky Mountains, *in* Can. J. Earth Sci. 21, p. 1050-1060.

Ellen, Stephen, D., and Mark, Robert, K., 1993, Mapping debris flow hazard in Honolulu using a DEM, *in* Hydraulic Engineering, 1993, p. 1774-1779.

Florence, Paolo, Billi, 1993, Steep mountain streams: processes and sediment, *in* Z. Geomorph. N. F., Suppl. -Bd. 88, p. 1-16.

Gadd, Ben, 1995, Handbook of the Canadian Rockies, Corax press, Jasper, Canada, 831p.

Gardner, James, S., and Jones, Norman K., 1993, Sediment transport and yield at the Raikot glacier, Nanga Parbat, Punjab Himalaya, *in* Himalaya to the sea, Routledge, London, p. 184-197.

Gardner, James, S., 1986, Sediment movement in ephemeral streams on mountain slopes, Canadian Rocky Mountains, *in* Abrahams, Athol, D., ed., Hillslope Processes, Binghamton Symposia in Geomorphology: International Series, No. 16, Allen & Unwin, Inc., Winchester, p.97-113.

Gardner, James, S., 1982, Alpine mass-wasting in contemporary time: some examples from the Canadian Rocky Mountains, *in* Thorn, Colin, E., ed., Space and Time in Geomorphology 1ST ed., George Allen and Unwin, Ltd., London, p. 171-192.

Gardner, James, S., 1981a, Ephemeral and episodic transport of debris on mountain slopes, *in* Progress report on research conducted under permit from Parks Canada, Western Region Parks Canada, Calgary, 22p.

Garland, Gerald, G., and Olivier, Mervin, J., 1993, Predicting landslides from rainfall in a humid, sub-tropical region, *in* Geomorphology, Vol. 8, p. 165-173.

Halladay, I. A. R., and Mathewson, D. H., eds., 1971, A guide to the geology for the Eastern Cordillera along the Trans-Canada Highway between Calgary, Alberta and Revelstoke, British Columbia, The Alberta Society of Petroleum Geologists, Canadian exploration frontiers, Banff, 96p.

Hearn, G., and Jones, D. K. C., 1986, Geomorphology and mountain highway design: some lessons from the Dharan-Dhankuta highway, east Nepal, *in* Int. Geomorph. Part I, John Wiley & Sons Ltd., New York, p. 203-219.

Henz, J. F., 1972, An operational technique of forecasting thunderstorms along the lee of a mountain range, *in* J. of Applied Meteorology, Vol. 11, p. 1284-1292.

Hungr, Oldrich, Morgan, G. C., VanDine, D. F., and Lister, D. R., 1987, Debris flow defenses in British Columbia, *in* Geological Soc. Of America Rev. in Eng. Geology, Vol. VII, p. 201-222.

Hungr, O., and Morgan, G. C., 1984, Quantitative analysis of debris torrent hazards for design of remedial measures, *in* Can. Geotech. J., Vol. 21, p. 663-677.

Innes, John, L., 1983, Debris Flows, *in* Progr. Phys. Geogr. Vol. VII, p.469-501.

Irigaray, C., Fernandez, T., and Chacon, J., 1994, GIS landslide inventory and analysis of determinant factors in the sector of Rute (Cordoba, Spain), *in* 7th International IAEG Congress: Balkema, Rotterdam, p. 4659-4668.

Jackson, Jr., L. E., Hungr, O., Garnder, J. S., and MacKay, C., 1989, Cathedral mountain debris flows, Canada, *in* Bull. of the Int. Assoc. of Eng. Geology, No. 40, p. 35-54.

Jackson, Jr., L. E., 1987, Debris flow hazard in the Canadian Rocky Mountains, Geological survey of Canada, 86-11, 10p.

Jackson, Jr., L. E., Kostaschuk, R. A., and MacDonald, G. M., 1987, Identification of debris flow hazard on alluvial fans in the Canadian Rocky Mountains, *in* Geological Soc. of Am. Rev. in Eng. Geology, Vol. VII, p. 115-124.

Janz, B., and Storr, D., 1977, The climate of the contiguous mountain Parks, *in* Atm. Env. Service, Environment Canada, Toronto, p. 83-88.

Johnson, A. M., 1970, Physical processes in geology, Freeman, Cooper, San Francisco.

Kostaschuk, R. A., MacDonald, G. M., and Putman, P., 1986, Depositional process and alluvial fan-drainage basin morphometrc relationships near Banff, Alberta, Earth Surface Processes and Landforms, Vol. 11, p. 471-484.

Lee, Fitzhugh, T., Odum, Jack, K., and Lee, John, D., 1994, Rockfalls and debris avalanches in the Smugglers Notch area, Vermont, US Geological Survey Bulletin, 2075, 33p.

Lillesand, Thomas, M., and Kiefer, Ralph W., 1994, Remote sensing and image interpretation 3RD ed., John Wiley & Sons, Inc., New York, 750p.

Luckman, Brian, H., 1997, Developing a proxy climate record in the Canadian Rockies: some problems and opportunities, *in* Climatic Change, Vol. 36, 1997, p.223-244.

Lueder, Donald, R., 1959, Aerial Photographic Interpretation - Principles and Applications, McGraw-Hill Book Company, Inc., New York, 462p.

Maddox, R. A., Canova, F., and Hoxit, L. R., 1977b, Meteorological characteristics of flash flood events over the western United States, *in* Mountain Weather Rev., Vol. 108, p. 1866-1877.

Major, Jon, J., 1997, Depositional processes in large-scale debris-flow experiments, *in* The J. of Geology, Vol. 105, p. 345-366.

Melton, M. A., 1965, The geomorphic and paleoclimatic significance of alluvial deposits in southern Arizona, *in* J. of Geology, Vol. 73, p. 1-38.

Natural Resources Canada, 1989, Ecological Land Classification of Banff National Park.

Neary, D. G., and Swift Jr., L. W., 1987, Rainfall thresholds for triggering a debris avalanching event in the southern Appalachian Mountains, *in* Geological Soc. Of America, Rev. in Eng. Geology, Vol. VII, p.81-92.

Okuda, S., Suwa, H., Okunishi, K., Yokoyama, K., and Kyoto, M., Nakano, 1980, Observations on the motion of a debris flow and its geomorphological effects, *in* Z. Geomorph. N. F., Suppl. -Bd. 35, p. 142-163.

Orville, H. D., 1968, Ambient wind effects on the initiation and development of cumulus clouds over mountains, *in* J. of Atmospheric Sci., Vol. 25, p. 385-403.

Osterkamp, W. R., Hupp, C. R., and Blodgett, J. C., 1986, Magnitude and frequency of debris flows, and areas of hazard on Mount Shasta, Northern California, US Geological Survey professional paper, 1396-C, 21p.

Page, Robert, Bayley, Suzanne, Cook, Douglas, Green, Jeffrey, E., and Ritchie, Brent, J. R., 1996, Banff-Bow valley study: At the crossroads, Minister of Supply and Services Canada.

Parks Canada, 1998, Summary weather data for Banff National Park, Internet, http://vertex.worldweb.com/ParksCanada-Banff/weather.html.

Phillips, Christopher, J., and Davies, Timothy, R. H., 1988, Generalized viscoplastic modeling of debris flow, *in* J. of Hydraulic Eng., 115, p. 1160-1163.

Price, R., Simony, P., Cook, D., Balkwill, H., and Ghent, E., 1971, Geologic guidebook to the Canadian Cordillera Between Calgary, Alberta and Revelstoke, British Columbia, Geological Society of America, field trip #3, Rocky Mountain Section Meeting, Calgary, 76p.

Podor, Andrew, Paul, 1992, Recent debris flow frequency and magnitude at West Wilson Creek, Banff National Park, Alberta, *unpublished Masters thesis*, University of Waterloo, Ontario, 211p.

Pole, Graeme, 1993, Canadian Rockies, Altitude publishing, Banff, Canada, 348p.

Public Works, Canada, 1981, Proposed improvements to the Trans-Canada Highway in Banff National Park, kms. 13 to Sunshine Road, Environmental impact statement, Vol. 1, p. 4-8.

Rapp, Anders, and Nyberg, Rolf, 1981, Alpine debris flows in Northern Scandinavia, *in* Geografiska Annaler, Vol. 63A, p.183-196.

Rebetez, Martine, Lugon, Ralph, and Baeriswyl, Pierre-Alain, 1997, Climatic change and debris flows in high mountain regions: The case study of the Ritigraben torrent (Swiss Alps), *in*, Climatic Change, Vol. 36, 1997, p.139-157.

Rowbotham, David, M., 1995, Applying GIS to modeling of slope stability in Phew Tal watersheds, Nepal, *unpublished Ph.D. thesis*, University of Waterloo, Ontario.

Saczuk, Eric, A. R., 1996, Mapping geomorphic hazard sites using GIS between Bow Pass and Seebe in southwestern Alberta, *unpublished Honours thesis*, University of Mantioba, Winnipeg, 56p.

Sauchyn, Mary, A., 1983, Evaluation of botanical methods for dating debris flow deposits and estimating debris flow hazard in the Canadian Rocky Mountains, *unpublished Masters thesis*, University of Waterloo, Ontario, 147p.

Schumm, S. A., 1963, The Disparity between present rates of denudation and orogeny, *in* Erosion and Sediment Yield, 1982, Benchmark Papers in Geology/63, Hutchinson Ross Publishing Company, Stroudsburg, Pennsylvania, 375p.

Selby, M. J., 1991, Earth's changing surface: An introduction to geomorphology, Clarendon press, Oxford, 607p.

Selby, M. J., 1982, Hillslope materials and processes, Oxford University press, Oxford, 264p.

Shlemon, Roy, J., Wright, Robert, H., and Montgomery, David, R., 1987, Anatomy of a debris flow, Pacifica, California, *in* Geological Soc. Of America, Rev. in Eng. Geology, Vol. VII, p.181-199.

Slaymaker, Olav, 1990, Natural hazards in mountain terrain: Howe Sound, British Columbia: Field Tour, Canadian Association of Geographers, Western Division Annual Meeting March 10-11, 1990, University of British Columbia, 53p.

Spurr, Stephen, H., 1960, Photogrammetry and Photo-Interpretation, The Ronald Press Company, New York, 472p.

van Steijn, Henk, 1995, Debris-Flow magnitude-frequency relationships for mountainous regions of Central and Northwestern Europe, *in* Geomorphology, Vol. 15, p.259-273.

Suwa, H., and Kyoto, S., Okuda, 1980, Dessection of valleys by debris flows, *in* Z. Geomorph. N. F., Suppl. -Bd. 35, p. 164-182.

Takahashi, T., 1981, Debris flow, *in* Annual Rev. of Fluid Mechanics, Vol. 13, p. 57-77.

Takahashi, T., 1979, Study on the deposition of debris flow due to abrupt change of bed slope, *in* Disaster Prevention Research Annuals, Kyoto University, #22 B-2.

Thurber Consultants Ltd., 1985a, Cathedral Mountain debris flow, Report to CP Rail special projects, 37p.

Thurber Consultants Ltd., 1985b, Final report: Debris torrent assessment, Wahleach and Floods, Highway 1; Hope to Boston Bar Creek Summit, Coquihalla Highway, report prepared for British Columbia Ministry of Transportation and Highways, Victoria.

Trenhaile, Alan S., 1990, The geomorphology of Canada; an introduction, Oxford University Press, Toronto, Ontario.

VanDine, D. F, 1985, Debris flow and debris torrents in Southern Canadian Cordillera, *in* Can. Geotech. J., Vol. 22, p. 44-68.

Vuichard, Daniel, 1986, Geological and petrographical investigations for the mountain hazards mapping project, Khmbu Himal, Nepal, *in* Mountain Research and Development, Vol. 6, No. 1, p. 41-52.

Whalley, W. B., 1974, The mechanics of high magnitude, low-frequency rock failure, *in* Geographical Papers, University of Reading, 27p.

Whipple, Kelin X., 1997, Open-channel flow of Bingham fluids: Applications in debris-flow research, *in* The J. of Geology, Vol. 105, p. 243-262.

Whipple, K., and Dunne, T., 1992, The influence of debris-flow rheology on fan morphology, Owens Valley, California, *in* Geol. Soc. Am. Bull., Vol. 104, p. 887-900.

Whittow, John, 1984, Dictionary of physical geography, Penguin books, London, 591p.

Wieczorek, Gerald, F., 1987, Effect of rainfall intensity and duration on debris flows in central Santa Cruz Mountains, California, *in* Geological Soc. of Am. Rev. in Eng. Geology, Vol. VII, p. 93-104.

Sources of Personal Communication

Abbott, Harold	Yoho National Park Warden, Yoho National Park, British Columbia.
Barber, David G.	Professor of Geography University of Manitoba, Winnipeg, Manitoba.
Campbell, Michael	Professor of Recreational Studies University of Manitoba, Winnipeg, Manitoba.
Gardner, James, S.	Vice-President Academic and Professor of Geography University of Manitoba, Winnipeg, Manitoba.
Lastra, Rod	Master of Science (Botany) student University of Manitoba, Winnipeg, Manitoba.
Pacas, Charlie	Banff National Park Warden, Banff, Alberta.
deScally, Fes	Professor of Geography Okanagan University College, Kelowna, British Columbia.
Teller, Jim T.	Professor of Geological Sciences University of Manitoba, Winnipeg, Manitoba.

Appendix 1

Id	Site	C	East	North	D_{CH}	W_{CI}	L_{CI}	D_{CI}	D_{DI}	A_{CI}	A_{DI}	V_{CI}	V_{DI}	A_{RI}	Mode 2	Mode 1	Ecoregion	Soils	Vegetation	Land	A	S	E_{min}	E_{max}	Relief	Basin A	r
1	N93-5*	1.0	499458E	5777950N	2.0	7.0	2,093	3.5	1.5	14,651	6,279	51,279	9,419	746,608	53	28	U. Subalpine*	Brunisol, Regosol*	Avalanche*	Colluvial Rubble*	32.1*	3.5*	2,071*	2,802*	731*	878,124	0.78
2	N93-6*	1.0	500514E	5776187N	2.5	18.0	1,435	9.0	6.7	25,830	19,229	613,000	128,834	829,204	47	High Hazard	Alpine*	Rock*	Unvegetated*	Rock*	61.6*	15.5*	1,925*	3,042*	1,117*	859,552	1.20
3	N93-9		510766E	5763849N	2.0	6.0	728	3.0	1.0	4,368	1,456	13,104	1,456	657,628	60	Low Hazard	Alpine	Brunisol, Regosol	Open Mixed Coniferous	Glacier	230.9	24.8	1,709	2,958	1,249	692,452	1.50
4	N93-10	5.0	511088E	5762746N	2.5	19.0	2,328	9.5	7.0	44,232	32,592	420,204	228,144	2,180,176	18	High Hazard	Alpine	Brunisol, Regosol	Pine/Buffalo berry	Rock	144.2	34.5	1,694	2,953	1,259	2,323,268	0.83
5	N93-11	1.0	511452E	5762326N	2.0	13.5	2,260	6.8	2.5	20,340	11,300	91,530	28,250	773,940	51	High Hazard	Alpine	Brunisol, Regosol	Open Mixed Coniferous	Glacier	152.8	29.7	1,582	3,220	1,638	895,644	1.73
6	N93-12	1.0	511995E	5761350N	3.0	14.0	1,985	7.0	4.0	27,790	15,880	194,530	63,520	535,468	73	High Hazard	Alpine	Brunisol, Regosol	Open Mixed Coniferous	Glacier	133.3	24.2	1,597	3,045	1,448	618,404	1.84
7	N93-13		512608E	5760594N	1.0	2.5	1,565	1.3	0.3	3,913	783	4,891	196	351,608	112	Low Hazard	Alpine	Brunisol, Regosol	Open Mixed Coniferous	Glacier	114.7	39.2	1,686	2,999	1,313	419,332	2.03
8	N93-14	2.0	513184E	5759971N	2.5	10.0	1,118	5.0	2.5	11,180	5,590	55,900	13,975	573,372	68	21	Alpine	Brunisol, Regosol	Open Mixed Coniferous	Colluvial Rubble	160.8	41.3	1,695	2,947	1,252	607,780	1.61
9	N93-18	2.5	519833E	5753492N	2.0	13.0	2,108	6.5	4.5	27,404	18,972	178,126	85,374	1,739,464	23	High Hazard	Alpine	Brunisol, Regosol	Spruce-Fir	Rock	172.7	40.8	1,511	3,285	1,774	1,874,496	1.30
10	N93-19	2.5	519513E	5754622N	1.5	22.0	2,520	11.0	9.5	55,440	47,880	609,840	454,860	1,703,220	23	High Hazard	Alpine	Brunisol	Spruce-Fir	Rock	235.6	36.1	1,561	3,274	1,713	1,827,268	1.27
11	N93-21	1.0	520319E	5750449N	2.0	9.0	1,370	4.5	2.5	12,330	6,850	55,485	17,125	1,179,392	33	5	Alpine	Brunisol> Luvisol	Pine/Buffalo berry	Rock	201.0	35	1,636	3,086	1,450	1,267,020	1.29
12	N93-22	1.0	521198E	5749027N	2.5	12.0	1,300	6.0	3.5	15,600	9,100	93,600	31,850	169,956	231	High Hazard	Alpine	Regosol	Pine/Buffalo berry	Rock	208.2	34.2	1,640	2,711	1,071	233,012	2.22
13	N93-26	3.5	521276E	5748769N	2.0	17.0	1,908	8.5	6.5	32,436	24,804	275,706	161,226	324,232	121	High Hazard	Alpine	Brunisol	Pine/Buffalo berry	Rock	237.0	31.9	1,656	2,856	1,200	993,792	1.91
14	N93-29	1.5	527404E	5741435N	2.0	8.0	1,838	4.0	2.0	14,704	7,352	58,816	14,704	661,936	59	16	Alpine	Brunisol, Regosol	Pine/Buffalo berry	Rock	144.2	34.5	1,694	2,953	1,259	772,212	1.43
15	N93-33	3.0	531751E	5734911N	2.0	15.0	2,305	7.5	5.5	34,575	25,358	259,313	139,453	574,692	68	High Hazard	Alpine	Brunisol, Regosol	Spruce-Fir	Rock	157.4	27.9	1,748	2,866	1,118	687,836	1.35
16	N93-34	1.5	531082E	5734765N	1.0	10.0	2,193	5.0	4.0	21,930	17,544	109,650	70,176	1,181,104	33	High Hazard	Alpine	Brunisol, Regosol	Open Mixed Coniferous	Rock	174.6	27.9	1,758	2,857	1,099	1,316,004	0.96
17	N93-40	3.0	547805E	5717035N	3.0	9.0	1,093	4.5	1.5	9,837	3,279	44,267	4,919	986,420	40	30	Alpine	Brunisol, Regosol	Avalanche	Rock	218.4	30.2	1,859	2,889	1,030	1,030,104	1.01
18	N93-41	1.0	547805E	5715667N	2.0	6.5	1,340	3.3	1.3	8,710	3,350	28,308	4,188	334,348	117	93	Alpine	Brunisol, Regosol	Heath Tundra	Rock	227.2	34.5	1,878	3,083	1,205	389,156	1.93
19	N93-42	1.0	547873E	5715116N	2.0	8.5	1,343	4.3	2.3	11,416	6,044	48,516	13,598	419,548	93	30	Alpine	Brunisol, Regosol	Heath Tundra	Rock	198.0	26.8	1,838	3,036	1,198	493,720	1.70
20	1A-1	1.0	592862E	5669498N	2.0	6.0	2,038	3.0	1.0	12,228	4,076	36,684	4,076	1,222,280	32	26	U. Subalpine	Brunisol, Regosol	Open Mixed Coniferous	Rock	153.6	31.2	1,402	2,635	1,233	2,923,464	0.72
21	1A-3	1.5	589691E	5670383N	1.5	8.0	2,680	4.0	2.5	21,440	13,400	85,760	33,500	1,568,196	25	High Hazard	U. Subalpine	Brunisol, Regosol	Open Mixed Coniferous	Colluvial> Rock	227.1	31.1	1,407	2,765	1,358	3,058,604	0.78
22	1A-4	2.5	587651E	5672696N	3.5	15.2	1,320	7.6	4.1	20,064	10,824	152,486	44,378	1,307,560	30	High Hazard	U. Subalpine	Brunisol, Regosol	Open Mixed Coniferous	Colluvial> Rock	222.5	31.7	1,414	2,637	1,223	3,561,152	0.65

* Release areas for sites N93-5 and N93-6 are not entirely within the boundaries of Banff National Park. Therefore the GIS layer data is not accurate for these two sites

Explanation of database variables are found on the following page.

Appendix 1

Explanation of Database Variables

Variable	Explanation	Units
Id	An integer value, which is used to link the sites database entry with its polygon on the GIS map in Appendix 2.	N/A
Site	An identifier which was used to locate a site in the field.	N/A
C	Diameter of the culvert pipe for each site if a culvert was present.	Meters
East	UTM Easting value for the location where the debris flow channel comes into contact with the highway.	UTM
North	UTM Northing value for the location where the debris flow channel comes into contact with the highway.	UTM
D_{Cel}	Depth of the channel as measured from the top of the debris to the banks not including levees, if present.	Meters
W_{Cl}	Width of the channel as measured between the banks.	Meters
L_{Cl}	Length of channel as measured from digitized aerial photographs.	Meters
D_{Cl}	Depth of channel computed as $0.5 \times W_{Cl}$.	Meters
D_{Dl}	Depth of debris in the channel computed as $D_{Cl} - D_{Cel}$.	Meters
A_{Cl}	Area of channel computed as $W_{Cl} \times L_{Cl}$.	Meters^2
A_{Dl}	Area of debris in the channel computed as $0.5 \times D_{Dl} \times L_{Cl}$.	Meters^2
V_{Cl}	Volume of channel computed as $W_{Cl} \times D_{Cl} \times L_{Cl}$.	Meters^3
V_{Dl}	Volume of debris in the channel computed as $1.5 \times D_{Dl} \times L_{Cl}$.	Meters^3
A_{Rl}	Area of release region as measured from digitized aerial photographs.	Meters^2
Mode 1	Recurrence interval model Mode 1 results for each site.	Numerical data is in years.
Mode 2	Recurrence interval model Mode 2 results for each site.	Years.
Ecoregion	Ecoregion that is dominant for each site based on data extracted from the Ecoregion GIS layer.	N/A
Soils	Dominant soils below tree line for each site based on data extracted from the Soils GIS layer.	N/A
Vegetation	Dominant vegetation below tree line for each site based on data extracted from the Vegetation GIS layer.	N/A
Land	Dominant landform for each site based on data extracted from the Landforms GIS layer.	N/A
A	Mean aspect of each site based on data extracted from the Aspect GIS layer.	Degrees
S	Mean slope of each site based on data extracted from the Slope GIS layer.	Degrees
E_{Min}	Minimum elevation of each site based on data extracted from the Digital Elevation Model (DEM) GIS layer.	Meters
E_{Max}	Maximum elevation of each site based on data extracted from the Digital Elevation Model (DEM) GIS layer.	Meters
Relief	Relief of each site computed as $E_{Max} - E_{Min}$.	Meters
Basin A	Area of each site as measured from digitized aerial photographs.	Meters^2
r	Melton's ruggedness number for each site computed as Relief x Basin $A^{-0.5}$.	N/A

Appendix 2

The base map shown here is a combination of an aspect layer and a digital elevation model layer of Banff National Park.

The colored areas represent each of the 22 debris flow sites. GIS software assigns a unique integer value to each site based on its color. The integer values are then linked with the database entry for that site.

Appendix 3

The images below show the cropped debris flow sites with red representing the release are and orange representing the debris flow channel.

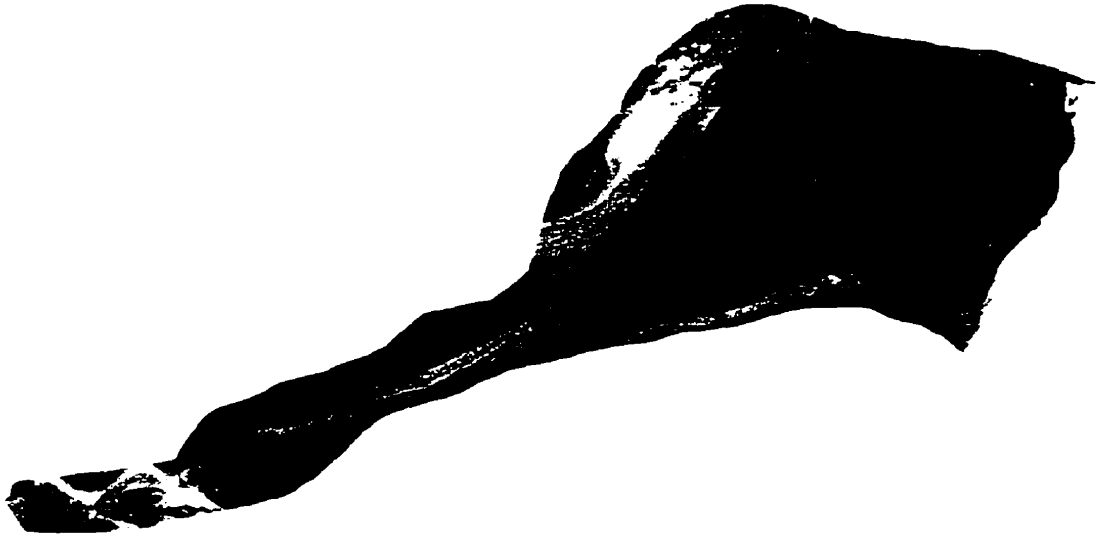

Site N93-5.

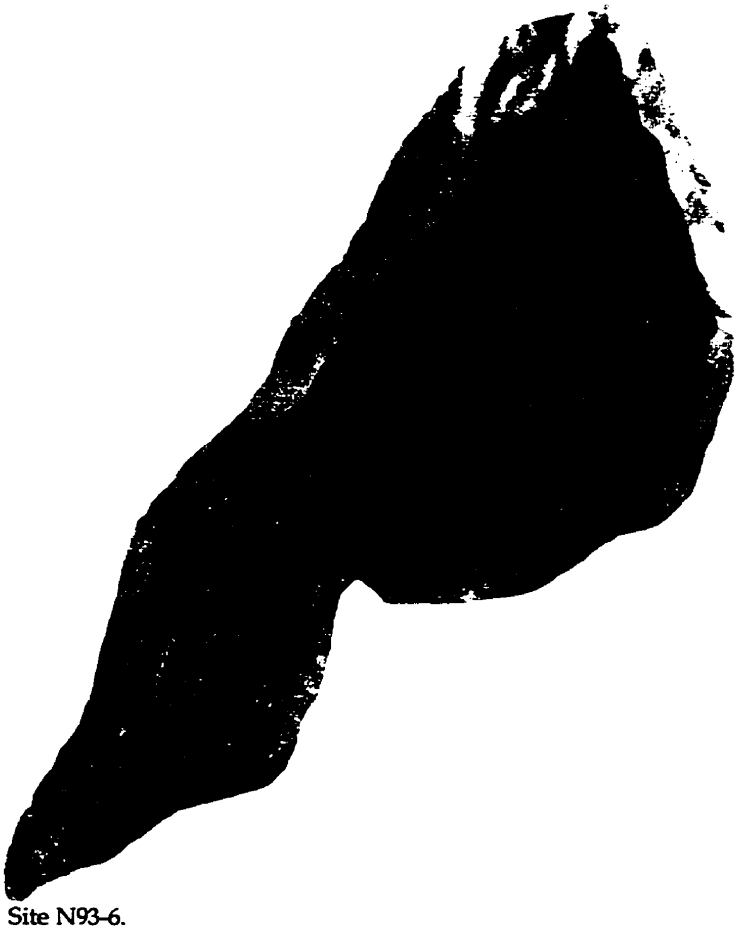

Site N93-6.

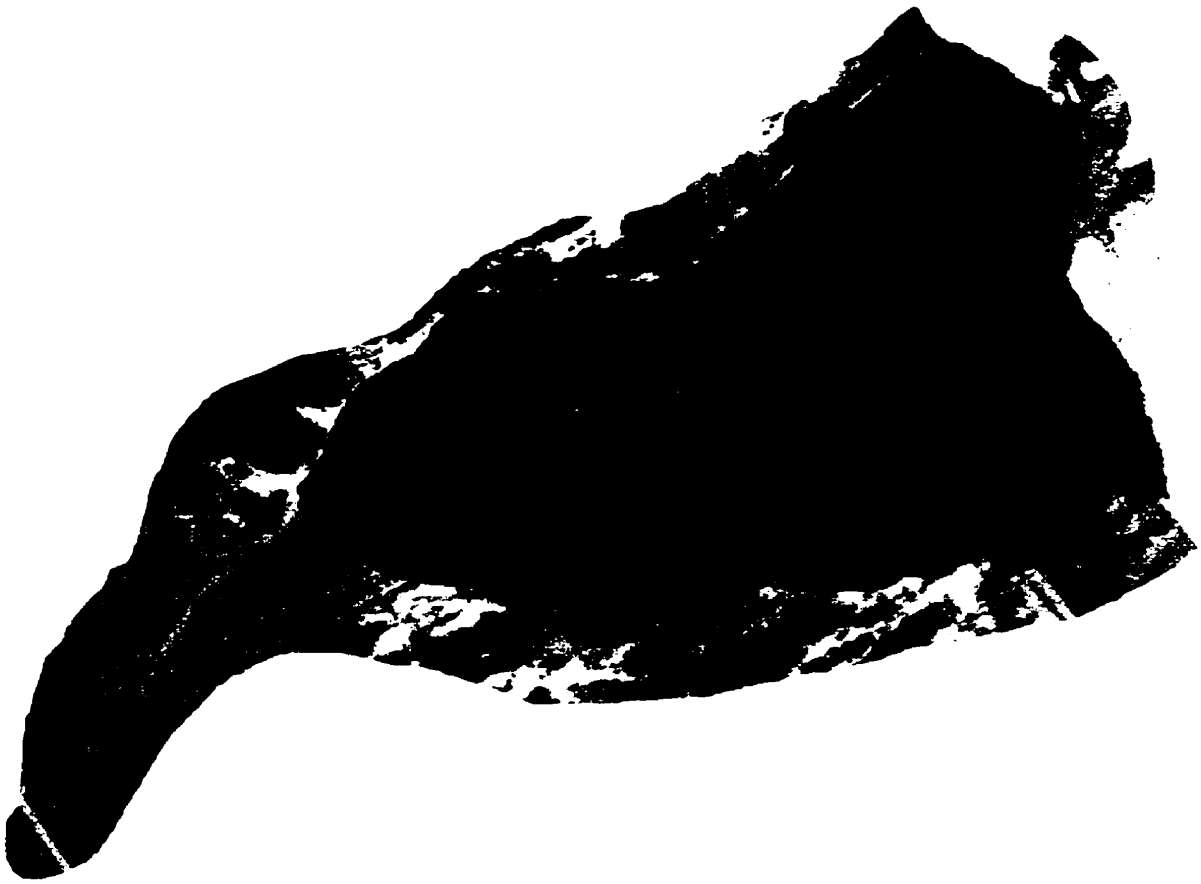

Site N93-9.

Site N93-10.

Site N93-11.

Site N93-12.

Site N93-13.

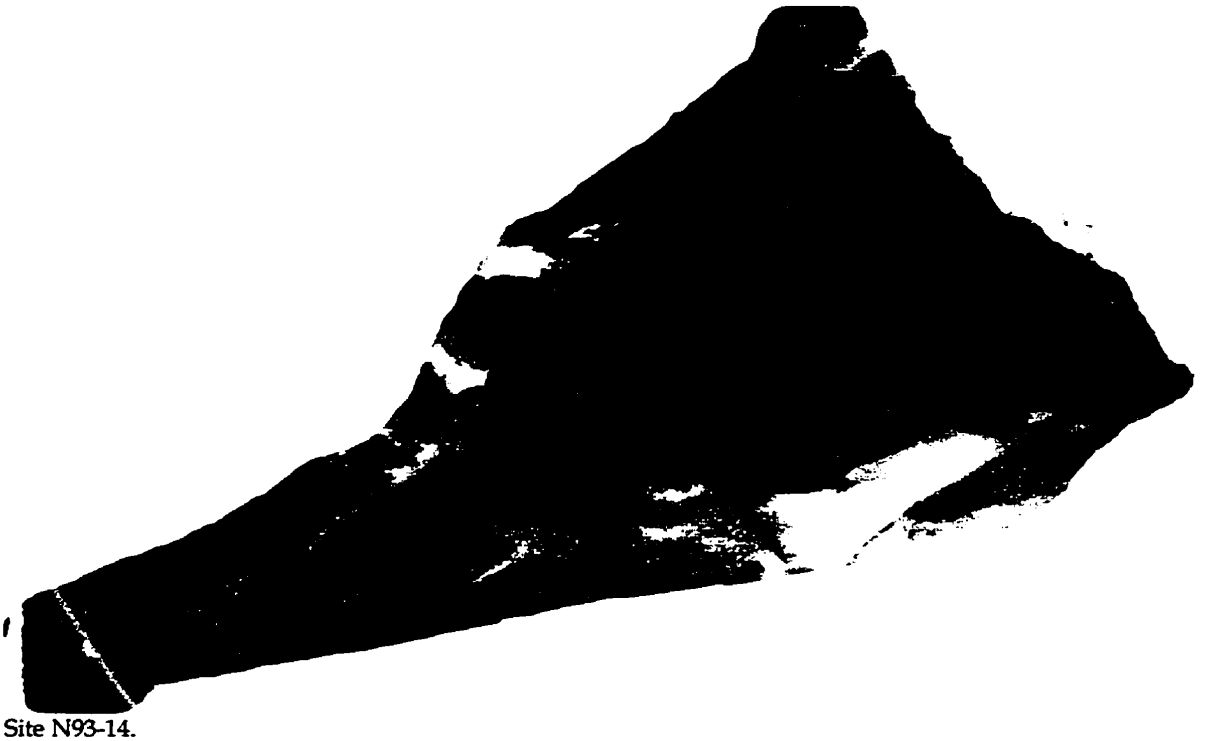

Site N93-14.

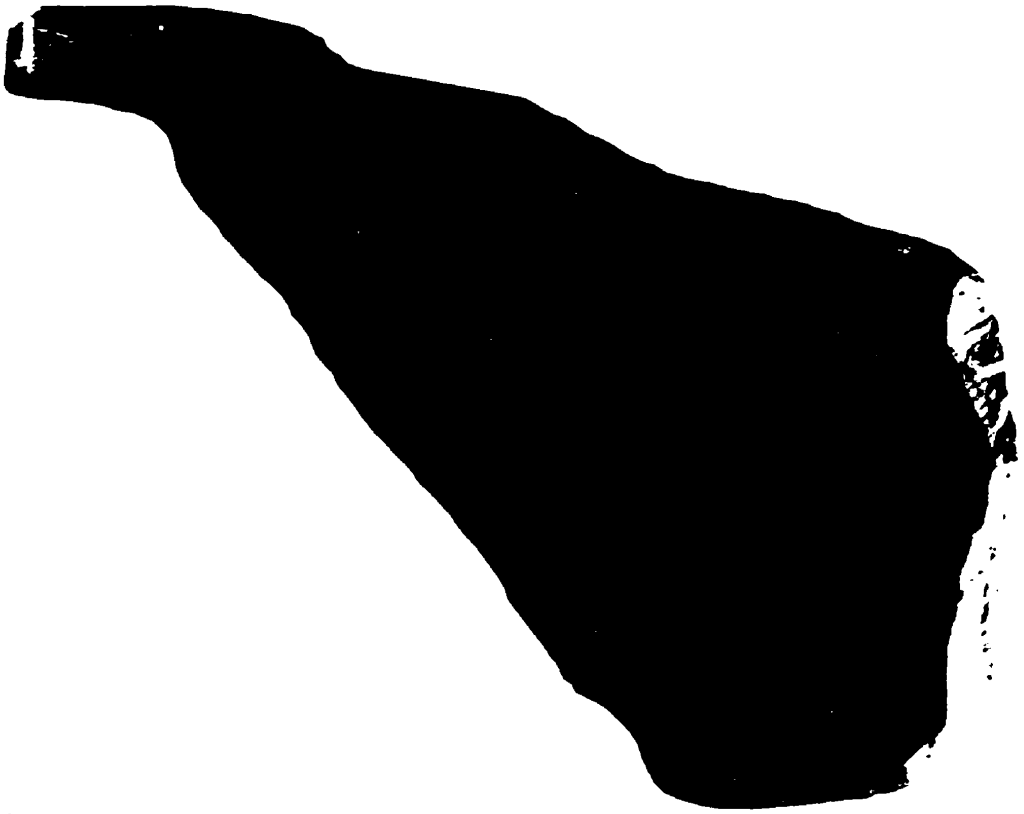

Site N93-18.

Site N93-19.

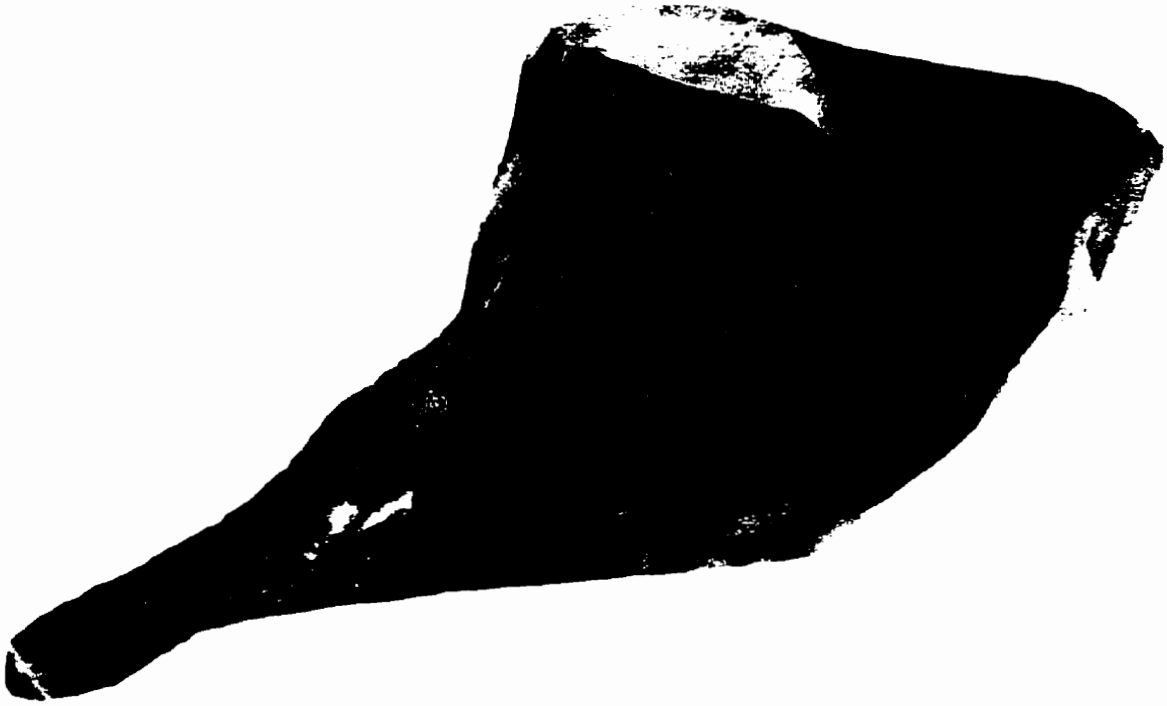

Site N93-21.

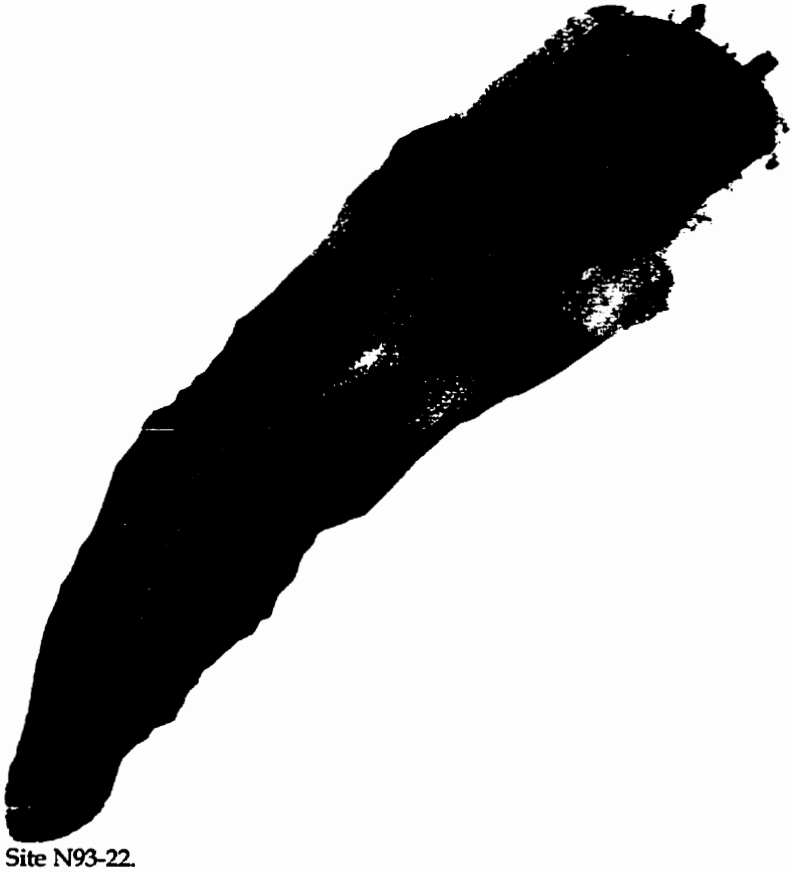

Site N93-22.

Site N93-24.

Site N93-29.

Site N93-33.

Site N93-34.

Site N93-40.

Site N93-41.

Site N93-42.

Site 1A-4.

Site 1A-1.

Site 1A-3.

IMAGE EVALUATION TEST TARGET (QA-3)

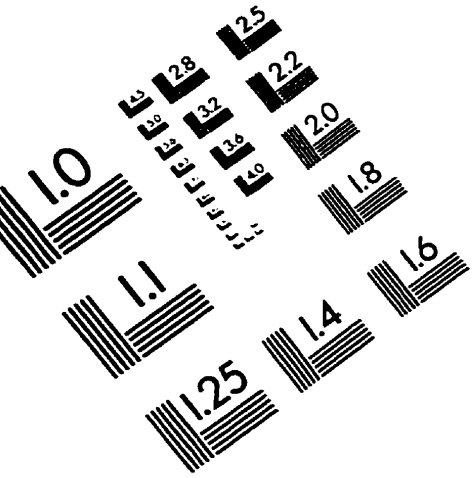

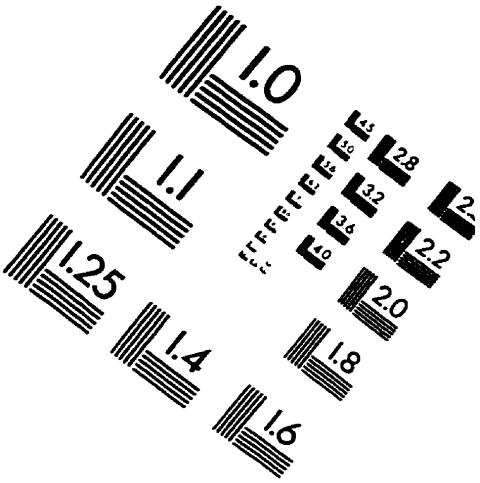

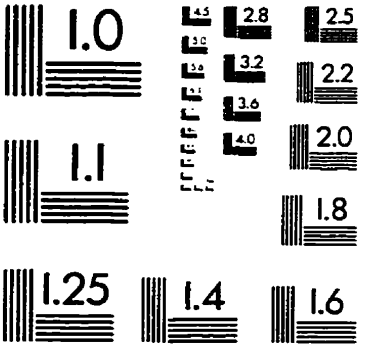

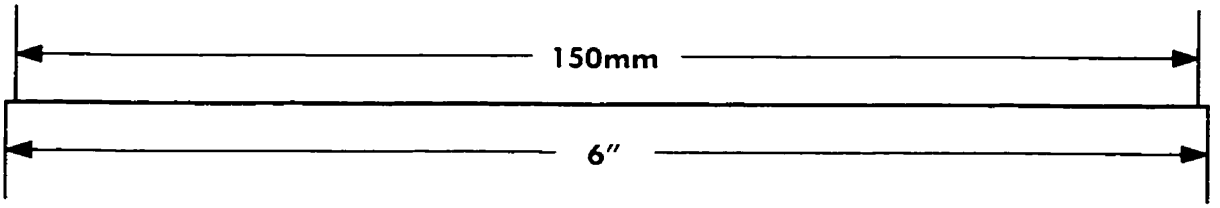

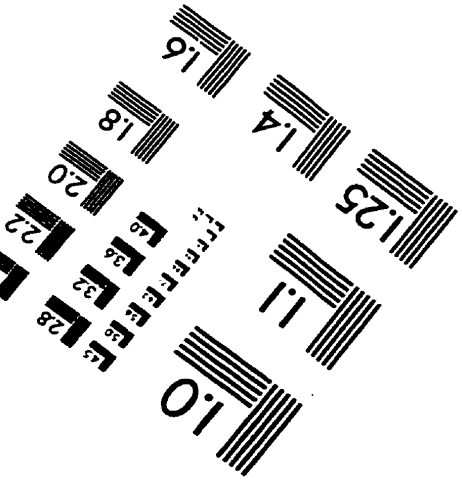

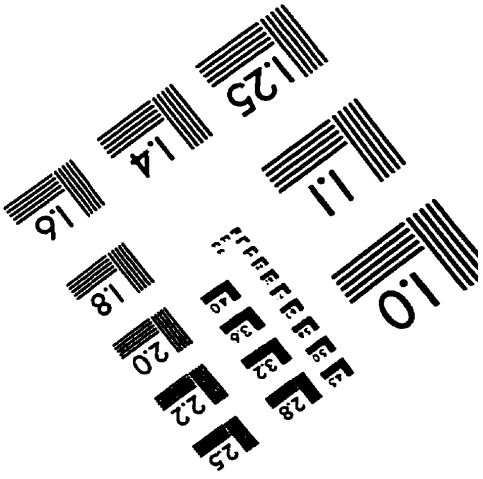

APPLIED IMAGE, Inc
1653 East Main Street
Rochester, NY 14609 USA
Phone: 716/482-0300
Fax: 716/288-5989